Inorganic Chemistry

Article

pubs.acs.org/IC

Conformational Landscapes of Metal(II) Porphyrinato, Chlorinato, and Morpholinochlorinato Complexes

Meenakshi Sharma,[†,§] Alexander L. Ticho,[†,‡,§] Lalith Samankumara,[†,⊥] Matthias Zeller,[∥,¶] and Christian Brückner*[,†]

[†]Department of Chemistry, University of Connecticut, Unit 3060, Storrs, Connecticut 06269-3060, United States

[∥]Department of Chemistry, Youngstown State University, One University Plaza, Youngstown, Ohio 44555-3663, United States

Supporting Information

ABSTRACT: The macrocycle conformation of [*meso*-tetraarylporphyrinato]metal complexes is metal-dependent. Furthermore, hydroporphyrins and some of their analogues are known to be more conformationally flexible than the parent porphyrins, but the extent to which this is reflected in their metal-dependent conformations was much less studied. *meso*-Tetraarylmorpholinochlorins are intrinsically nonplanar chlorin analogues in which the five-membered pyrroline moiety was replaced by a six-membered morpholine moiety. The metal complexes (M = Ni^{2+}, Cu^{2+}, Zn^{2+}, Pd^{2+}, Ag^{2+}) of *meso*-aryl-2,3-dimethoxychlorins and *meso*-arylmorpholinochlorins were prepared. Their conformations were determined using X-ray crystal structure diffractometry and compared against those of their free bases, as well as against the conformations of the corresponding metalloporphyrins. Out-of-plane displacement plots visualized and quantified the conformational changes upon stepwise conversion of a pyrrole moiety to a dimethoxypyrroline moiety and to a dialkoxymorpholine moiety, respectively. The generally nonplanar macrocycle conformations were found to be central-metal-dependent, with the smaller ions showing more nonplanar conformations and with the metallomorpholinochlorins generally showing a much larger conformational range than the corresponding metallochlorins, which, in turn, were more nonplanar than the corresponding porphyrins. This attests to the larger conformational flexibility of the morpholinochlorin macrocycle compared to that of a chlorin or even a porphyrin macrocycle. The degree of nonplanarity affects the electronic structure of the metal complexes, as can also be seen in a comparison of their UV−vis spectra. We thus further define the conformational and electronic effects governing pyrrole-modified porphyrins.

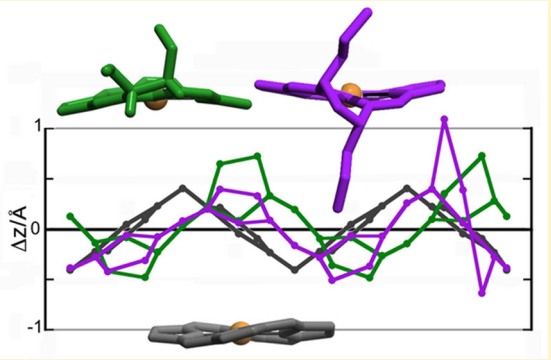

INTRODUCTION

Synthetic porphyrins, chlorins (2,3-dihydroporphyrins), and their analogues,[1] as their free bases or metal complexes, are widely investigated for their utility in a number of technical applications, such as small-molecule-activation catalysts,[2] components in functional devices,[3] or light-harvesting dyes.[4] Their singlet oxygen sensitization and other photophysical properties also lead to their recommendation in medical applications such as photochemotherapeutics,[5] optical labels,[6] or imaging agents.[7] The ability to adjust the electronic (optical) properties of the chromophores is crucial for these applications. This tuning can be accomplished by, for instance, extension of the π conjugation of the chromophore by fusion to conjugated substituents,[8] in rare cases by the change of the *meso*-aryl substituents,[9] by adjustment of the planarity of the chromophore,[10] or through the adjustment of their degree of saturation (i.e., the conversion of porphyrins → chlorins → bacteriochlorins or isobacteriochlorins).[1,11] Generally, chlorins and bacteriochlorins absorb light more intensely at longer wavelengths relative to porphyrins,[5b,11] and nonplanar chromophores absorb at longer wavelengths than their planar analogues.[12]

Multiple examples of *meso*-arylporphyrinoids derived by the formal replacement of a pyrrole of a porphyrin by a nonpyrrolic moiety were reported.[1,13] One example containing a five-membered carbacycle in place of a pyrrole is the azuliporphyrin **1**, exclusively prepared by total synthesis.[14] A formal replacement of a β,β' bond by a lactone moiety results in the formation of the porpholactones **2**, generated by carefully calibrated oxidations of porphyrins or chlorins.[15] The oxypyriporphyrin **3** containing a six-membered nonpyrrolic heterocycle can be accessed using either total synthesis or porphyrin modification methodologies.[16] The oldest example containing a six-membered heterocycle is the lactone **4**, discovered as a fortuitous product along a nongeneralizable reaction pathway.[17]

Received: March 31, 2017
Published: June 26, 2017

DOI: 10.1021/acs.inorgchem.7b00799
Inorg. Chem. 2017, 56, 11490−11502

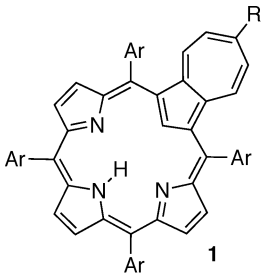

1

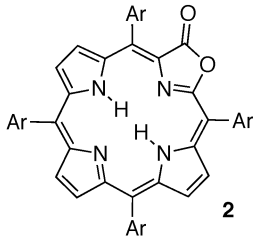

2

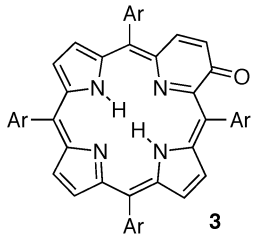

3

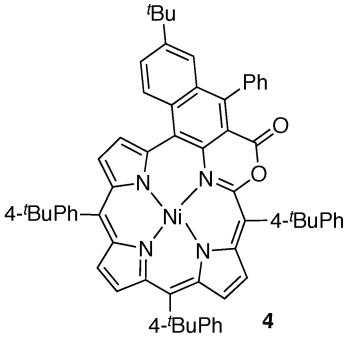

4

We contributed by the introduction of a facile ring-expansion reaction of 2,3-dihydroxychlorins to generate morpholinochlorins, such as the free base $\mathbf{5H_2}$ or nickel complex **5Ni**.[18] Free-base morpholinochlorin was shown to possess a modestly ruffled conformation.[18c,d] The mode of deformation and its extent is dependent on the number and types of morpholine substituents or the presence of an intramolecular linkage at the ortho position of a *meso*-phenyl group (as in $\mathbf{6H_2}$).[18d] Mono- and bismorpholinobacteriochlorins **7** showed much more pronounced ruffled conformations,[19] and the origin of their conformation-dependent optical properties was studied.[20]

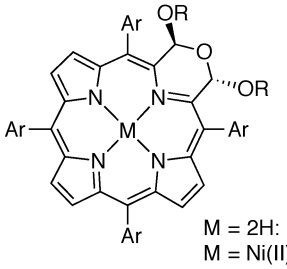

M = 2H: $\mathbf{5H_2}$
M = Ni(II): **5Ni**

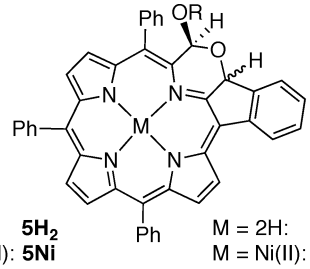

M = 2H: $\mathbf{6H_2}$
M = Ni(II): **6Ni**

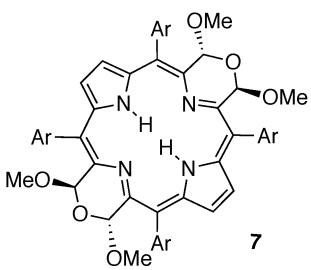

7

The [morpholinochlorinato]nickel(II) complex **5Ni**, driven by the small size of the square-planar-coordinated, diamagnetic d^8 ion, exhibits a significantly more ruffled conformation than the corresponding free base.[18a,d] [Morpholinochlorinato]nickel(II) complexes containing different types or numbers of morpholine substituents all assumed near-identical conformations, suggesting that the conformation of morpholinochlorins is primarily controlled by the presence of the central metal. In contrast, the conformation of the corresponding free bases varied widely.[18d,21] The conformational modulation of the electronic properties of natural and synthetic porphyrins through steric crowding of their periphery or through protein interactions is well-explored.[10,12ab,22] It is also known that the corresponding hydroporphyrins (and their analogues) are conformationally more flexible,[19,20,23] but how this increased flexibility is reflected in the conformation of various metal complexes of the hydroporphyrins has not been fully detailed. The broadened optical spectra of free-base morpholinochlorins,[18c] their substituent-dependent conformations, and the demonstration of the drastic conformational modulation of the morpholinochlorin free base upon metalation with Ni^{II} suggests that these chromophores are particularly flexible.[18d] However, aside from this lone example, the conformational landscape of the metal complexes of morpholinochlorins has not yet been systematically studied.

We detail here our investigation into the conformations and optical spectra of a series of metal(II) complexes of diethoxymorpholinochlorins (M = 2H, Ni^{2+}, Cu^{2+}, Zn^{2+}, Pd^{2+}, Ag^{2+}), as determined by their single-crystal X-ray structures. We compare their conformations to those of the corresponding 2,3-dimethoxychlorin and porphyrin complexes. We thus delineate the conformational landscape of the metallochlorins and metallomorpholinochlorins. Specifically, the comparison describes the extent that reduction of a single β,β' double bond and the insertion of an O atom into this double bond changes the conformational flexibility of the ligand. Last, a comparison of the UV−vis spectra of this series of compounds defines the extent of the electronic modulation that these chemical and conformational changes induce.

RESULTS AND DISCUSSION

Synthesis of the Metallochlorins and Metallomorpholinochlorins Investigated. The syntheses of free-base dimethoxychlorin $\mathbf{10H_2}$ and diethoxymorpholinochlorin $\mathbf{11H_2}$ followed established routes (Scheme 1).[18a,d,24] OsO_4-mediated dihydroxylation of free-base *meso*-tetraarylporphyrins $\mathbf{8H_2}$ converted them to the corresponding 2,3-*vic*-dihydroxychlorins $\mathbf{9H_2}$.[18a,24] These diols can be methylated using a classic Williamson ether synthesis, forming the 2,3-*vic*-dimethoxychlorins $\mathbf{10H_2}$[24] or ring-expanded to the morpholinochlorin $\mathbf{11H_2}$ carrying two ethoxy substituents in an anti configuration.[18a,d] The latter reaction involves oxidative cleavage of the diol functionality to the corresponding secochlorin bisaldehyde and an in situ ethanol-induced double acetal formation with concomitant intramolecular ring closure. The mechanism and origin of the stereoselectivity for the reaction are known.[18d]

The metal complexes were formed from the free-base chromophores using standard metal insertion reaction conditions: metal(II) salt, solvent, heat, and, in some cases, base, except the silver(II) complexes were formed in a disproportionation reaction using silver(I) acetate as the metal source.[25] Some insertions could also be accomplished under microwave-assisted conditions.[26] All compounds showed the expected spectroscopic and analytical properties.

The different *meso*-aryl groups used [phenyl, 4-methylphenyl, and 4-(trifluoromethyl)phenyl] had, as expected,[27] only a negligible effect on the electronic properties of the chromophores (see the Supporting Information for a direct comparison of the UV−vis spectra of pairs of matching chromophores carrying different *meso*-aryl substituents). Importantly, however, the solubility and crystallinity of the differently *meso*-aryl-substituted derivatives varied greatly. Generally, the phenyl-substituted derivatives ($\mathbf{X^{Ph}}$) generated well-soluble compounds but of relatively low propensity to form crystalline materials. The *p*-tolyl-derived compounds ($\mathbf{X^{CH_3}}$) were the least soluble of

DOI: 10.1021/acs.inorgchem.7b00799
Inorg. Chem. 2017, 56, 11490−11502

Scheme 1. Synthetic Pathways of the Metalloporphyrinoids Investigated, including the CCDC Code for the Known Metalloporphyrins Structures Used for Comparison[a]

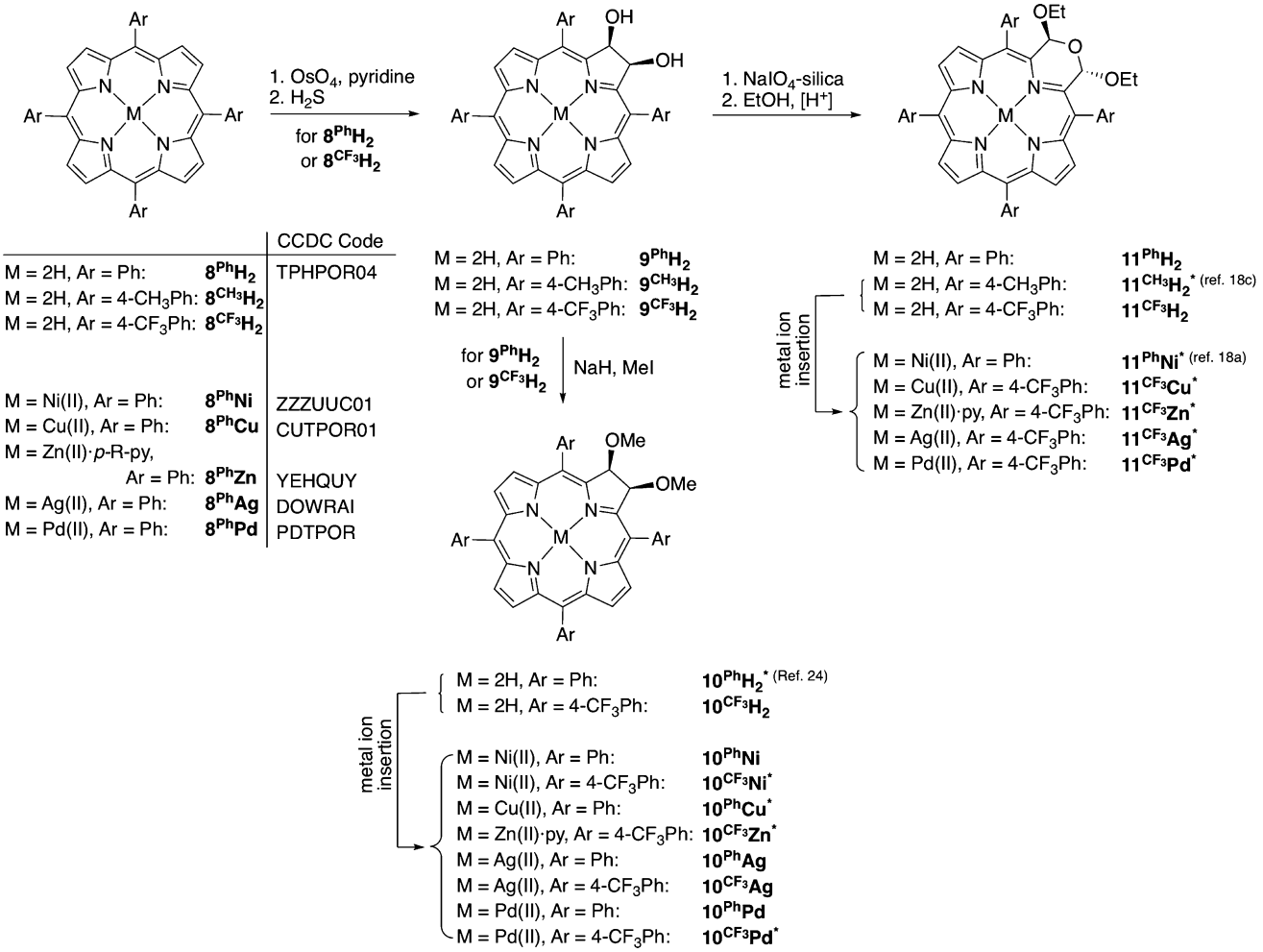

		CCDC Code
M = 2H, Ar = Ph:	$8^{Ph}H_2$	TPHPOR04
M = 2H, Ar = 4-CH_3Ph:	$8^{CH_3}H_2$	
M = 2H, Ar = 4-CF_3Ph:	$8^{CF_3}H_2$	
M = Ni(II), Ar = Ph:	$8^{Ph}Ni$	ZZZUUC01
M = Cu(II), Ar = Ph:	$8^{Ph}Cu$	CUTPOR01
M = Zn(II)·*p*-R-py, Ar = Ph:	$8^{Ph}Zn$	YEHQUY
M = Ag(II), Ar = Ph:	$8^{Ph}Ag$	DOWRAI
M = Pd(II), Ar = Ph:	$8^{Ph}Pd$	PDTPOR

M = 2H, Ar = Ph:	$9^{Ph}H_2$
M = 2H, Ar = 4-CH_3Ph:	$9^{CH_3}H_2$
M = 2H, Ar = 4-CF_3Ph:	$9^{CF_3}H_2$

M = 2H, Ar = Ph:	$11^{Ph}H_2$
M = 2H, Ar = 4-CH_3Ph:	$11^{CH_3}H_2$* (ref. 18c)
M = 2H, Ar = 4-CF_3Ph:	$11^{CF_3}H_2$
M = Ni(II), Ar = Ph:	$11^{Ph}Ni$* (ref. 18a)
M = Cu(II), Ar = 4-CF_3Ph:	$11^{CF_3}Cu$*
M = Zn(II)·py, Ar = 4-CF_3Ph:	$11^{CF_3}Zn$*
M = Ag(II), Ar = 4-CF_3Ph:	$11^{CF_3}Ag$*
M = Pd(II), Ar = 4-CF_3Ph:	$11^{CF_3}Pd$*

M = 2H, Ar = Ph:	$10^{Ph}H_2$* (Ref. 24)
M = 2H, Ar = 4-CF_3Ph:	$10^{CF_3}H_2$
M = Ni(II), Ar = Ph:	$10^{Ph}Ni$
M = Ni(II), Ar = 4-CF_3Ph:	$10^{CF_3}Ni$*
M = Cu(II), Ar = Ph:	$10^{Ph}Cu$*
M = Zn(II)·py, Ar = 4-CF_3Ph:	$10^{CF_3}Zn$*
M = Ag(II), Ar = Ph:	$10^{Ph}Ag$
M = Ag(II), Ar = 4-CF_3Ph:	$10^{CF_3}Ag$
M = Pd(II), Ar = Ph:	$10^{Ph}Pd$
M = Pd(II), Ar = 4-CF_3Ph:	$10^{CF_3}Pd$*

[a]Asterisks indicate the compounds for which the structures are described here.

the three derivatives used and readily formed microcrystalline materials but rarely formed crystals large enough for analysis by single-crystal diffractometry. Empirically, we found the *p*-(trifluoromethyl)phenyl-substituted derivatives ($\mathbf{X}^{CF_3}$) to possess slightly better solubility than their tolyl congeners but to often form well-developed single crystals suitable for single-crystal X-ray diffraction studies. This effect of the *meso*-aryl substituents is not unique to these chromophores.[28] Similarly, the unprotected chlorin diols **9M** did not crystallize well, whereas the dimethoxy derivatives **10M** did.[24] Nonetheless, we were not able to generate crystals of $\mathbf{10}^{CF_3}\mathbf{Ag}$ suitable for single-crystal X-ray diffraction analysis.

Crystal Structures of the Metallochlorins. The crystal structure of the free-base chlorin $\mathbf{10}^{Ph}\mathbf{H_2}$ was reported previously.[24] It deviates slightly from planarity, as shown by the root-mean-square (rms) out-of-plane distortion of the $C_{20}N_4$ macrocycle from planarity [rms = 0.146 Å, with N−N distances of 4.194 Å ($N_{pyrrole\ H}$−$N_{pyrrole\ H}$) and 4.140 Å ($N_{pyrroline}$−$N_{pyrrole}$)], with the ruffled macrocycle distortions primarily originating from the nonplanar dimethoxypyrrolin moiety (Figures 1 and 2). This pyrroline distortion allows a more staggered conformation of the *vic-cis*-dimethoxy substituents.

All metallodimethoxychlorin structures are nonplanar, but to varying degrees in terms of the distortion mode (Figure 2) and extent of distortion, as expressed as the rms value of the deviation of the macrocycle heavy atoms from planarity (Figure 1). The pyrroline distortions that allow a staggered conformation of the two methoxy groups are maintained. Varying degrees of rotations around the $C_{pyrroline}$−OMe bonds allowed for different relative orientations of the two methoxy substituents; they may point to the same (e.g., for $\mathbf{10}^{CF_3}\mathbf{Pd}$) or opposite (e.g., for $\mathbf{10}^{Ph}\mathbf{Cu}$) general directions.

The metal type has a large influence on the conformation of these chlorins. As is frequently observed,[31] the small diamagnetic Ni^{II} d^8 ion (63 pm)[32] induces in $\mathbf{10}^{CF_3}\mathbf{Ni}$ the most severe ruffling in the tetrapyrrolic ligand. The ruffling distortion mode reduces the central cavity size, reducing the N−N distances to 3.849(5) Å ($N_{pyrrole}$−$N_{pyrrole}$) and 3.844(5) Å ($N_{pyrroline}$−$N_{pyrrole}$) while maintaining a near-perfect square-planar coodination environment.[23e] Compared to the conformation of the porphyrin complex $\mathbf{8}^{Ph}\mathbf{Ni}$, both the saddling and ruffling distortion modes are about twice as strongly expressed in the metallochlorin $\mathbf{10}^{CF_3}\mathbf{Ni}$. The biggest ion, the Pd^{II} ion (78 pm)[32] in $\mathbf{10}^{CF_3}\mathbf{Pd}$, causes among the square-planar complexes the least degree of distortion of the ligand and largely restores the metrics of the free-base ligand as the N−N distances widen to 4.042(5) and 4.033(4) Å ($N_{pyrroline}$−$N_{pyrrole}$ and $N_{pyrrole}$−$N_{pyrrole}$ are equivalent because of a 1:1 disorder of the pyrroline and pyrrole moieties).

DOI: 10.1021/acs.inorgchem.7b00799
Inorg. Chem. 2017, 56, 11490−11502

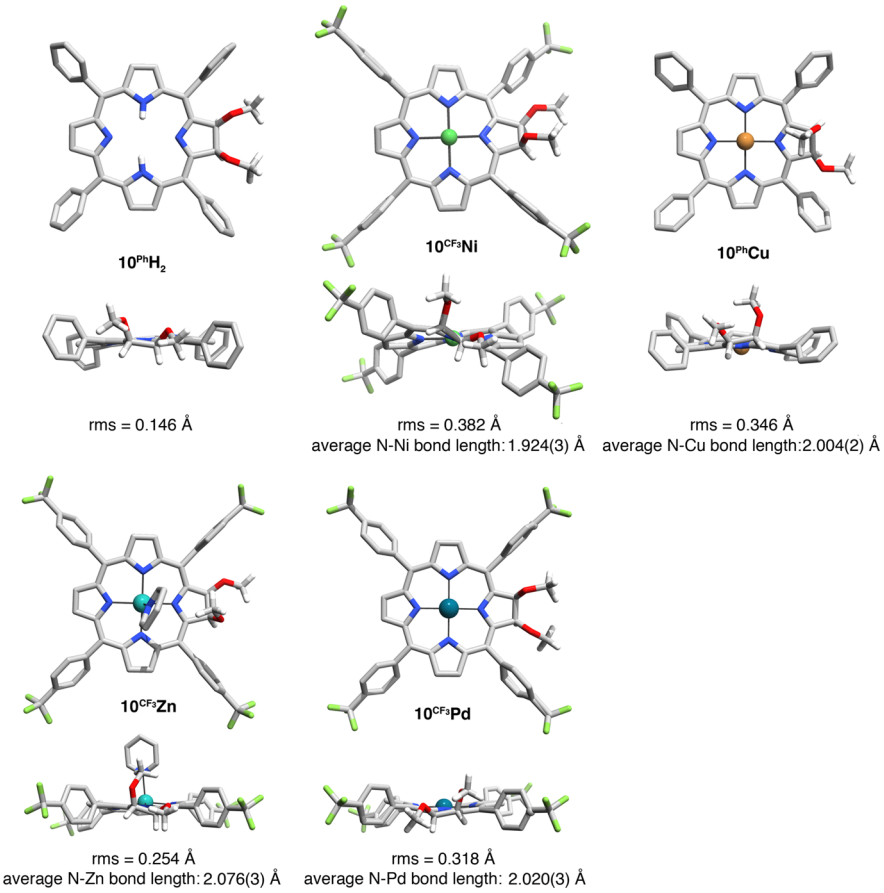

Figure 1. Stick presentations of the molecular structures of the dimethoxychlorins indicated, top and front views.[29] All H atoms attached to sp^2-hybridized C atoms, disorder and solvent, when present, were omitted for clarity; when several independent molecules in the unit cell were available, the one with the largest overall distortion was chosen. The rms values listed are the root-mean-square values of the deviation from planarity of the $C_{20}N_4$ macrocycle from planarity $[^1/_{24}(x_1^2 + x_2^2 + ... + x_{24}^2)]^{1/2}$. The N−M bond distances listed are the average of all four macrocycle bond distances. For details on the structural determinations, see Table 1 and the Supporting Information.

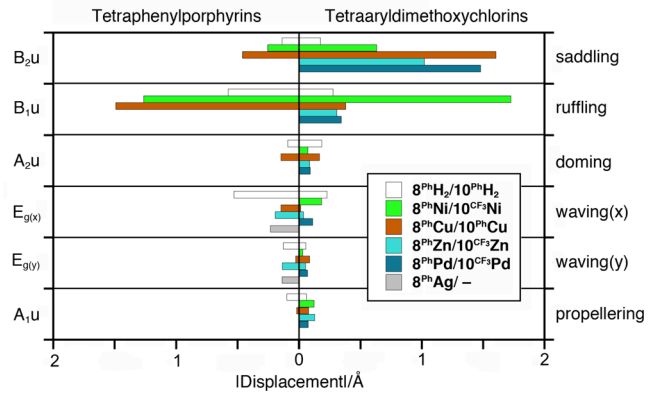

Figure 2. NSD analysis of the chromophore conformations in the (metallo)porphyrins and (metallo)chlorins indicated.[30] The absolute displacement value is plotted; for plots listing the positive/negative displacement values, see the Supporting Information.

The distortion mode of this metallochlorin is mostly saddled, with some ruffling contributions, whereas the corresponding porphyrin complex **8^{Ph}Pd** is idealized planar. The intermediate-sized (71 pm) copper(II)[32] complex **10^{Ph}Cu** assumes a modestly saddled conformation with some ruffling [with an $N_{pyrrole}$−$N_{pyrrole}$ distance of 3.973(3) Å and an $N_{pyrroline}$−$N_{pyrrole}$ distance of 4.033(3) Å]. This conformation for **10^{Ph}Cu** is an inversion of the conformation observed for **8^{Ph}Cu** (mostly ruffled and little saddled). The Zn^{II} ion (74 pm)[32] in **10^{CF_3}Zn** is also axially coordinated by pyridine, resulting in a square-pyramidal coordination geometry and causing some out-of-macrocycle plane coordination of the metal and some saddling and minor ruffling contributions to the ligand conformation. The Zn atom is drawn by the axial pyridine ligand out of the macrocycle plane, with the Zn atom protruding from the mean plane of the macrocycle N atoms by 0.322(1) Å. This leads to relatively long N−N bond lengths [an $N_{pyrrole}$−$N_{pyrrole}$ distance of 4.039(3) Å and an $N_{pyrroline}$−$N_{pyrrole}$ distance of 4.163(4) Å)]. In comparison, the conformation of **8^{Ph}Zn** is much more planar.

The dimethoxychlorin complex conformations observed here are all generally in line with expectations.[31] Their relevance lies in providing reference structures for the metallomorpholinochlorins that are derived from the metallochlorins by the formal insertion of an O atom between the pyrroline β-C atoms, and a change of the relative stereochemistry of the two alkoxy substituents from cis to trans, with no other change to the porphyrinic π system.

Crystal Structures of the Metallomorpholinochlorins. The formal replacement of a pyrroline in the free base **10^{Ph}H$_2$** by a morpholine moiety in the free base **11^{CH_3}H$_2$** slightly increases the overall nonplanarity of the macrocycle (Figure 3). The intraring N−N distances are long (an $N_{pyrrole}$−$N_{pyrrole}$ distance of 4.136 Å and an $N_{morpholine}$−$N_{pyrrole}$ distance of 4.240 Å); i.e., the inner cavity was slightly elongated compared to the corresponding dimethoxychlorin **10^{Ph}H$_2$**. The cavity of the

DOI: 10.1021/acs.inorgchem.7b00799
Inorg. Chem. 2017, 56, 11490−11502

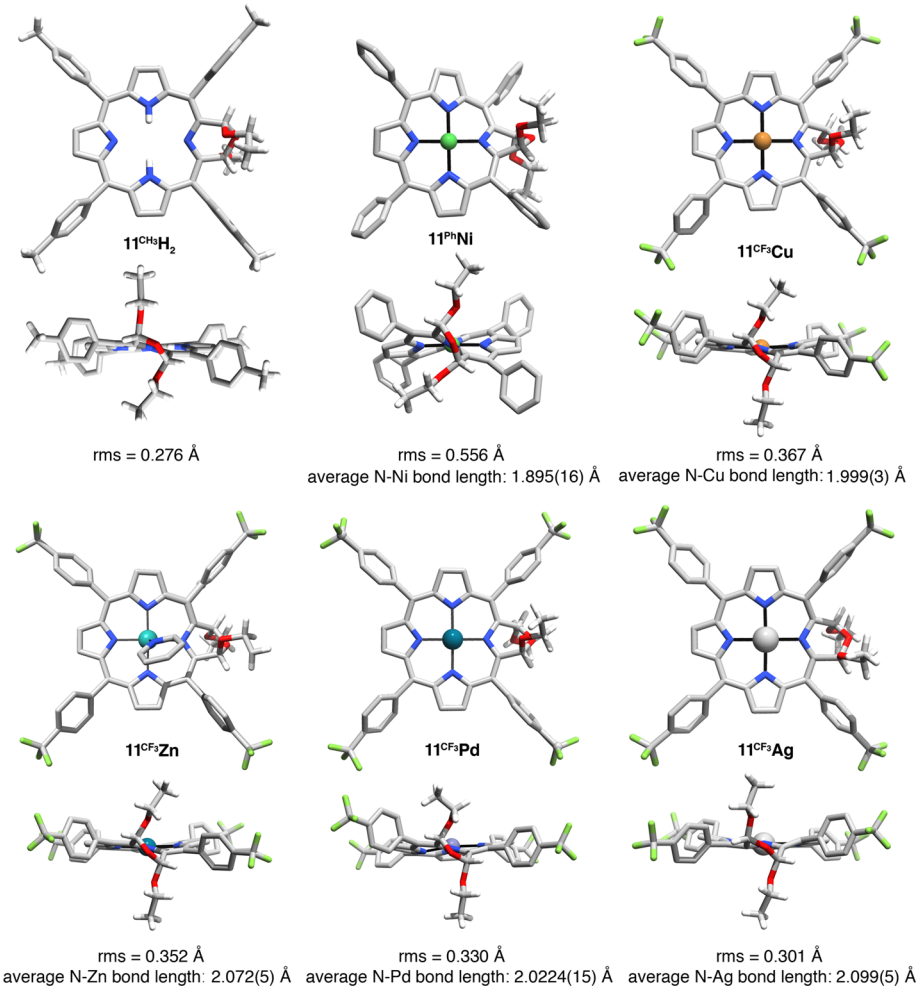

Figure 3. Stick presentations of the molecular structures of the morpholinochlorins indicated, top and front views.[29] We chose arbitrarily only the *M* isomer of the two helimeric enantiomers present in the unit cells. All H atoms attached to sp^2-hybridized C atoms, disorder and solvent, when present, were omitted for clarity; likewise, the axial pyridine ligand present in **11**^{CF_3}**Zn** was removed from the side view. The rms values listed are the root-mean-square values of the deviation from planarity of the $C_{20}N_4$ macrocycle from planarity $[^1/_{24}(x_1^2 + x_2^2 + ... + x_{24}^2)]^{1/2}$, i.e., omitting the morpholinochlorin O atoms from that determination. The N−M bond distances listed are the average of all four macrocycle bond distances. For details on the structural determinations, see Table 1 and the Supporting Information.

chlorin is itself slightly larger than the corresponding distances in the porphyrin **8**^{Ph}**H**$_2$ [4.194 Å ($N_{pyrrole\ H}$−$N_{pyrrole\ H}$) and 4.042 Å ($N_{pyrrole}$−$N_{pyrrole}$)]. The conformation of the nonpyrrolic and partially sp^3-hybridized building block in **11**^{CH_3}**H**$_2$ is decidedly nonplanar.[18c,d]

As observed and rationalized before,[18a,d,21] the corresponding nickel(II) complex **11**^{Ph}**Ni** is ruffled to an extraordinarily large degree, resulting in very short Ni−N bond distances [or, in other words, a small inner cavity, with an $N_{pyrrole}$−$N_{pyrrole}$ distance of 3.787(2) Å and an $N_{morpholine}$−$N_{pyrrole}$ distance of 3.793(2) Å]. This is remarkable because generally the M−N bond distances in the metallomorpholinochlorins are larger than those in the corresponding metallochlorins. Unfortunately, a normal-mode structural decomposition (NSD) analysis of the conformations of the morpholinochlorins using the same algorithm as that developed for a D_{4h} porphyrin macrocycle reference structure is not possible.[30,33]

The general metal-dependent trends seen in the [dimethoxychlorinato]metal structures before are preserved metallomorpholinochlorins, but the extent of the distortions are magnified. The most planar structure with the longest intraring N−N distances is **11**^{CF_3}**Ag** coordinating the largest metal ion, Ag^{II} (93 pm)[32] [an $N_{pyrrole}$−$N_{pyrrole}$ distance of 4.148(6) Å and an $N_{morpholine}$−$N_{pyrrole}$ distance of 4.272(7) Å]. Thus, coordination to Ag^{II} elongates the macrocycle cavity beyond the dimensions found in the free base. The next-largest ion, Pd^{II}, in **11**^{CF_3}**Pd** delivers $N_{pyrrole/morpholine}$−$N_{pyrrole}$ distances of 4.0420(45) and 4.0333(42) Å, which, however, cannot be assigned to one bond type or the other because of a disorder of the pyrrole/morpholine moiety with shared N atoms. The copper(II) and zinc(II) complexes in **11**^{CF_3}**Cu** and **11**^{CF_3}**Zn** again exhibit intermediate deformations that look mostly ruffled but with the Zn^{II} ion much less pulled out-of-plane by the axial pyridine than in the correspondng chlorin complex **10**^{CF_3}**Zn**. While zinc(II) complexes of porphyrins are generally readily prepared and stable,[25] **11**^{CF_3}**Zn** was curiously difficult to prepare and purify, suggesting a much larger lability of the axial ligand or the metal itself than in the corresponding complexes **8**^{Ph}**Zn** and **10**^{CF_3}**Zn**.

Comparison of the Conformational Trends Seen in the Metalloporphyrins, Metallochlorins, and Metallomorpholinochlorins. Out-of-plane displacement plots the porphyrin, chlorin, and morpholinochlorin structures allow a direct and semiquantitative comparison of their conformations (Figure 4). For any given metal ion, the degree of nonplanarity increases in the order porphyrin < chlorin < morpholinochlorin, reflecting

DOI: 10.1021/acs.inorgchem.7b00799
Inorg. Chem. 2017, 56, 11490−11502

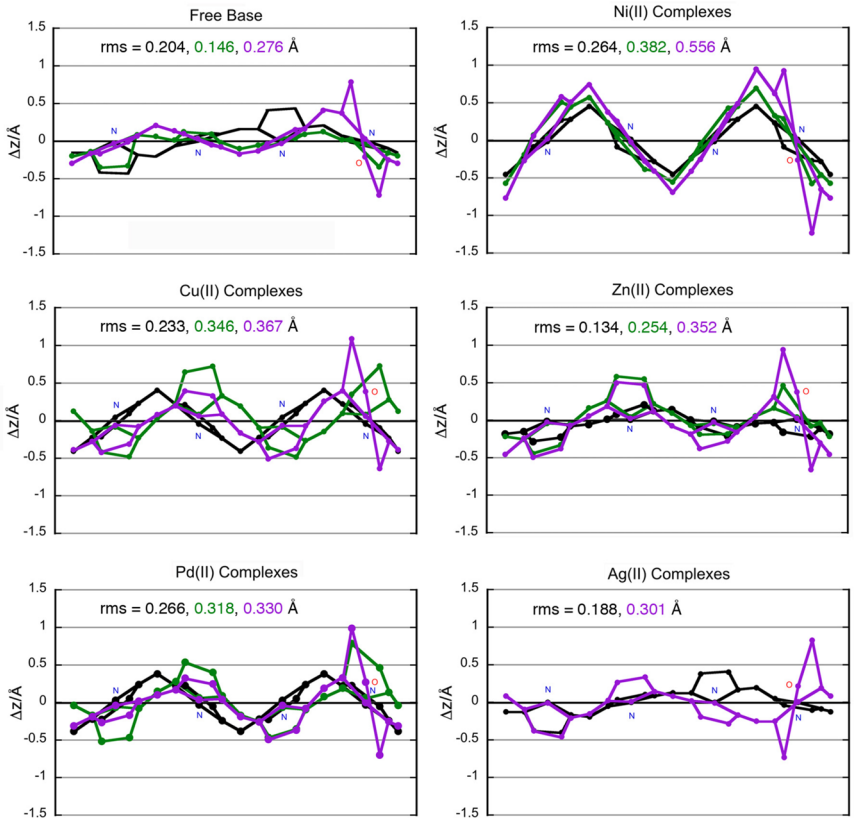

Figure 4. Out-of-plane displacement plots of the porphyrin (black), chlorin (green), and morpholinochlorin (purple) macrocycles of the experimentally determined conformations of the series of compounds indicated. The displacement is calculated based on a deviation from the least-squares plane calculated by the positions of the $C_{20}N_4$ macrocycles that are common to all compounds studied. For the definition of the rms values, see the caption to Figure 3. For details on the structural determinations, see Table 1 and the Supporting Information.

the increasing conformational flexibility of the macrocycles and the innate nonplanarity of their free-base compounds. In the free-base series, the predominant deformation modes change subtly from the porphyrin series to the hydroporphyrin series, from predominantly ruffling modes with some waving contribution to a mixture of conformational modes with no predominant deformation modes in the chlorin (compare also Figure 2) or the morpholinochlorin. All metal complexes are more nonplanar than their corresponding free bases. However, the individual conformational responses to a given metal ion vary.

The copper(II) complexes shift from predominantly ruffling to predominantly saddling, with the two hydroporphyrins showing very similar trends. The largely planar zinc porphyrin distorts into largely saddling modes in the hydroporphyinatozinc complexes, while the slight waving distortions in the silver porphyrin give way to modest ruffled distortions in the morpholinosilver complex. All nickel(II) and palladium(II) complexes, on the other hand, remain similarly strongly ruffled, as is also indicated by their similar Pd/Ni–N bond distances.

Comparison of the UV–vis Spectra of the Metalloporphyrins, Metallochlorins, and Metallomorpholinochlorins. The UV–vis spectra of the free-base compounds, chlorin, and morpholinochlorin reflect their porphyrin-like ($\mathbf{8}^{\mathbf{Ph}}\mathbf{H}_2$) and chlorin-like ($\mathbf{10}^{\mathbf{Ph}}\mathbf{H}_2$ and $\mathbf{11}^{\mathbf{CH_3}}\mathbf{H}_2$) chromophores (Figure 5), whereby the morpholinochlorin spectrum is characterized by a general broadening and a ~30 nm red-shifted λ_{max} band, previously attributed to the conformational flexibility and nonplanarity of the chromophore, respectively.[18c] Importantly, the chlorin and morpholinochlorin chromophores possess identical 18 + 2 chlorin-type π systems. Thus, the differences seen in the UV–vis spectra of the (metallo)chlorins and (metallo)morpholinochlorins can be traced almost exclusively to their differing conformations (a small contribution of the ring O atom cannot be neglected).[20] We recently demonstrated for the related morpholinobacteriochlorins that two factors are responsible in equal proportion for their Q-band red shift:[20] distortion of the π system from planarity and, unexpectedly, the C_β–C_α–C_α–C_β dihedral angle within the morpholine moiety. We believe these relationships also hold for the morpholinochlorins, and the data presented here provide some evidence that this is indeed the case.

The UV–vis spectra of all metalloporphyrin complexes and all metallochlorin/morpholinochlorin complexes are typical for metalloporphyrins and metallochlorins, respectively.[34] In the copper(II), zinc(II), and palladium(II) complexes, their different optical spectra follow the trends seen in their free bases, reflecting their similar—but certainly not identical—conformations. However, two metal series, the nickel(II) and silver(II) complexes, do not follow this pattern. In the nickel(II) series, the spectra of the nickel(II) chlorin complex $\mathbf{10}^{\mathbf{CF_3}}\mathbf{Ni}$ and the nickel(II) morpholinochlorin $\mathbf{11}^{\mathbf{Ph}}\mathbf{Ni}$ vary significantly from each other, with the spectrum of the metallomorpholinochlorin being much more red-shifted, but their macrocycle conformations are nearly identical (Figure 4). Thus, the surprisingly large differences between their optical spectra are attributed to the larger C_β–C_α–C_α–C_β dihedral angle within the morpholine moiety (50°) than in the pyrroline moiety (15°).[20] Inversely, the spectra of the chlorinato- and morpholinochlorinatosilver(II)

DOI: 10.1021/acs.inorgchem.7b00799
Inorg. Chem. 2017, 56, 11490–11502

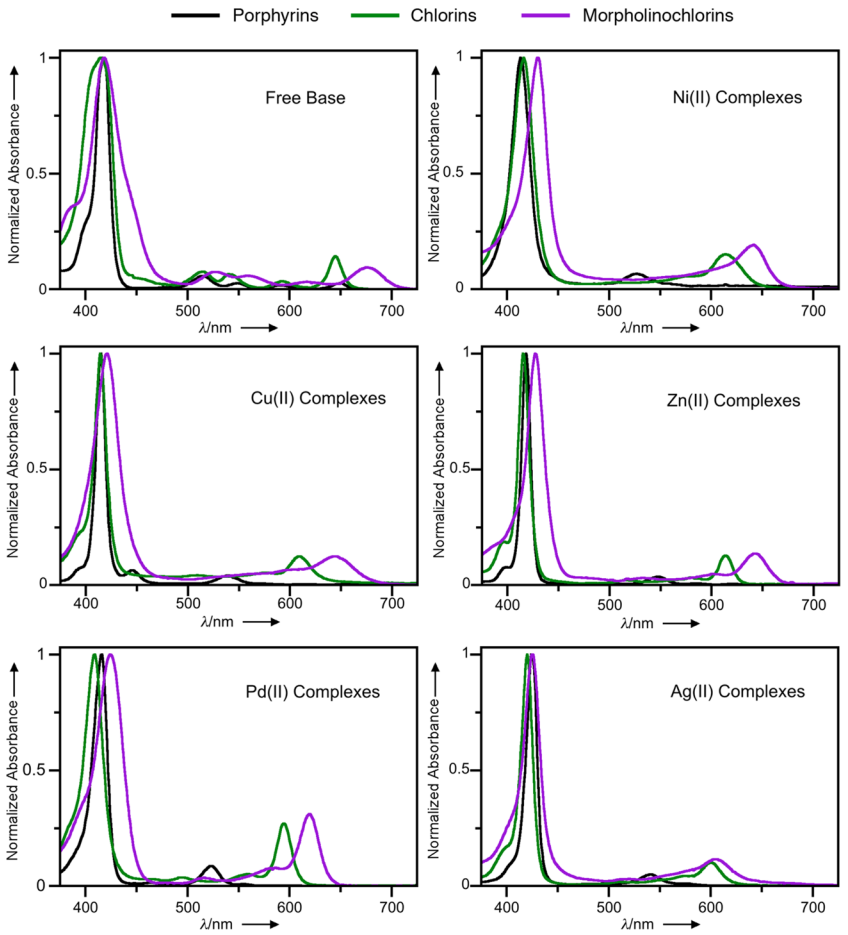

Figure 5. Comparison of the normalized UV−vis spectra of the *meso*-tetraphenylmetalloporphyrins, *meso*-tetrakis[4-(trifluoromethyl)phenyl]chlorins, and *meso*-tetrakis[4-(trifluoromethyl)phenyl]morpholinochlorins studied: black traces, metalloporphyrins; green traces, metallochlorins; purple traces, metallomorpholinochlorins.

complexes are very similar, suggesting similar conformations with similar $C_\beta-C_\alpha-C_\alpha-C_\beta$ dihedral angles, a proposition that, in the absence of the chlorinatosilver(II) crystal structure, could not be confirmed experimentally.

CONCLUSIONS

In conclusion, our investigation detailed the metal-dependent differences in the conformation of a series of metal(II) complexes of a *meso*-tetraphenylporphyrin, a *meso*-tetraarylchlorin, and a *meso*-tetraarylmorpholinochlorin. The greater nonplanarities of the metallochlorins compared to the corresponding metalloporphyrins are a clear indication for the greater conformational flexibility of the chlorin macrocycle, as observed previously.[31,35] Insertion of an O atom into the pyrroline moiety of the chlorins to formally generate the morpholinochlorins increases their inner cavity size and conformational flexibility. This leads to the formation of nonplanar metal complexes with comparably long N−M bonds, except in the case of the nickel(II) complexes, where the pure ruffling distortion decreases the M−Ni lengths with increasing deformation. The optical differences between porphyrins and chlorins are largey due to the presence of differing π electron chromophores (18 + 4 conjugated π electrons in porphyrins versus 18 + 2 conjugated π electrons in chlorins). On the other hand, the differences in the UV−vis spectra of the chlorins and morpholinochlorins possessing identical π systems can be traced to their differing conformations. In closing, this study further defines the conformational and electronic effects governing pyrrole-modified porphyrins.

EXPERIMENTAL SECTION

Materials. All solvents and reagents were used as received. Metalloporphyrins $\mathbf{8}^{\mathbf{Ph}}\mathbf{M}$,[25] free-base dihydroxychlorins $\mathbf{8}^{\mathbf{Ph}}\mathbf{H_2}$,[18a] $\mathbf{8}^{\mathbf{CH_3}}\mathbf{H_2}$,[15e,18c] and $\mathbf{8}^{\mathbf{CF_3}}\mathbf{H_2}$,[15e] dimethoxychlorin $\mathbf{10}^{\mathbf{Ph}}\mathbf{H_2}$,[24] morpholinochlorins $\mathbf{11}^{\mathbf{Ph}}\mathbf{H_2}$,[18c,d] and $\mathbf{11}^{\mathbf{CH_3}}\mathbf{H_2}$,[18c,d] metallomorpholinochlorin $\mathbf{11}^{\mathbf{Ph}}\mathbf{Ni}$,[18a] and the silica gel-supported $NaIO_4$[36] were prepared as described in the literature.

Preparation of Compounds. *[meso-Tetraphenyl-2,3-cis-dimethoxychlorinato]copper(II) (**10**$^{\mathbf{Ph}}$**Cu**).* To a solution of dimethoxychlorin ($\mathbf{10}^{\mathbf{Ph}}\mathbf{H_2}$; 12.0 mg, 1.77×10^{-5} mol) in CH_3Cl (10 mL) was added a solution of $Cu(OAc)_2 \cdot H_2O$ (11.0 mg, 5.32×10^{-5} mol) in methanol (MeOH; 2−3 mL). The reaction mixture was heated to reflux for 15 min. After the starting material was consumed [thin-layer chromatography (TLC) control], the reaction mixture was evaporated to dryness by rotary evaporation. The residue was dissolved in CH_2Cl_2 (15 mL) and washed with water (3 × 10 mL), and the organic phase was dried (Na_2SO_4), filtered, and concentrated by rotary evaporation. The residue was purified by column chromatography (silica−CH_2Cl_2/hexanes 1:1, gradient to pure CH_2Cl_2) to obtain $\mathbf{10}^{\mathbf{Ph}}\mathbf{Cu}$ (95% yield, 12.5 mg). $\mathbf{10}^{\mathbf{Ph}}\mathbf{Cu}$: MW = 738.35 g/mol; R_f = 0.57 (silica−CH_2Cl_2). UV−vis [CH_2Cl_2; λ_{max}, nm (log ε, M^{-1} cm^{-1}): 414 (5.33), 575 (sh), 610 (4.43). HR-MS (ESI^+, 100% CH_3CN, TOF). Calcd for $C_{46}H_{35}CuN_4O_2$ ($[M + H]^+$): m/z 738.2051. Found: m/z 738.2079.

*[meso-Tetraphenyl-2,3-cis-dimethoxychlorinato]nickel(II) (**10**$^{\mathbf{Ph}}$**Ni**).* To a solution of *meso*-tetrakis[4-(trifluoromethyl)phenyl]-2,3-*cis*-dimethoxychlorin ($\mathbf{10}^{\mathbf{Ph}}\mathbf{H_2}$; 15.0 mg, 2.22×10^{-5} mol) in C_6H_5CN

DOI: 10.1021/acs.inorgchem.7b00799
Inorg. Chem. 2017, 56, 11490−11502

(10 mL) was added 2−3 equiv of $Ni(OAc)_2·4H_2O$ (16 mg, 6.6×10^{-5} mol). The reaction mixture was refluxed for 20 min, and reaction progress was monitored by TLC. After the starting material was consumed, the reaction mixture was evaporated to dryness by rotary evaporation. The residue was dissolved in CH_2Cl_2 (15 mL) and washed with water (3 × 10 mL). The organic layer was dried (Na_2SO_4), filtered, and evaporated to dryness by rotary evaporation. The crude product was purified by column chromatography (silica−CH_2Cl_2/hexanes 1:1, gradient to pure CH_2Cl_2) to obtain **10^{Ph}Ni** (∼60% yield, 9−10 mg). **10^{Ph}Ni**: MW = 733.50 g/mol; R_f = 0.47 (silica−CH_2Cl_2). ^{1}H NMR (400 MHz, $CDCl_3$, 300 K): δ 8.32 (d, J = 4.9 Hz, 2H), 8.18 (s, 2H), 8.10 (d, J = 4.9 Hz, 2H), 7.86 (dd, J = 7.3 and 2.0 Hz, 4H), 7.66 (d, J = 6.3 Hz, 4H), 7.63−7.60 (m, 6H), 7.55−7.50 (m, 6H), 5.52 (s, 2H), 2.93 (s, 6H). ^{13}C NMR (100 MHz, $CDCl_3$, 300 K): δ 145.2, 141.5, 140.0, 139.7, 138.4, 137.7, 137.3, 136.9, 132.94, 132.90, 132.3, 128.9, 127.8, 127.5, 127.24, 127.16, 127.0, 123.9, 111.8, 83.9, 58.0. UV−vis [CH_2Cl_2; λ_{max}, nm (log ε, M^{-1} cm^{-1})]: 418 (5.08), 577 (sh), 613 (4.28). HR-MS (ESI$^+$, 100% CH_3CN, TOF). Calcd for $C_{46}H_{35}N_4NiO_2$ ([M + H]$^+$): m/z 733.2108. Found: m/z 733.2092.

*[meso-Tetraphenyl-2,3-cis-dimethoxychlorinato]silver(II) (**10^{Ph}Ag**).* To a solution of **$10^{Ph}H_2$** (20.0 mg, 2.95×10^{-5} mol) in C_6H_5CN (5 mL) was added AgOAc (17.0 mg, 1.03×10^{-4} mol). The reaction mixture was refluxed for 30 min and monitored by TLC. After the starting material was consumed, the reaction mixture was evaporated to dryness by rotary evaporation. The crude product was purified by column chromatography (silica−CH_2Cl_2/hexanes 1:1, gradient to pure CH_2Cl_2) to provide **10^{Ph}Ag** (44% yield, 10.0 mg). **10^{Ph}Ag**: MW = 782.67 g/mol; R_f = 0.45 (silica−CH_2Cl_2). UV−vis [CH_2Cl_2; λ_{max}, nm (log ε, M^{-1} cm^{-1})]: 421 (5.27), 576 (sh), 599 (4.27). HR-MS (ESI$^+$, 100% CH_3CN, TOF). Calcd for $C_{46}H_{35}AgN_4O_2$ ([M + H]$^+$): m/z 782.1805. Found: m/z 782.1794.

*[meso-Tetraphenyl-2,3-cis-dimethoxychlorinato]palladium(II) (**10^{Ph}Pd**).* To a solution of **$10^{Ph}H_2$** (20.0 mg, 2.95×10^{-5} mol) in C_6H_5CN (15 mL), was added $Pd(OAc)_2$ (38.0 mg, 1.18×10^{-4} mol). The reaction mixture was refluxed for 2−3 h and monitored by TLC. After the starting material was consumed, the reaction mixture was evaporated to dryness by rotary evaporation. The residue was dissolved in CH_2Cl_2 (15 mL) and washed with water (3 × 10 mL). The organic layer was dried (Na_2SO_4), filtered, and evaporated to dryness by rotary evaporation. The residue was purified by column chromatography (silica−CH_2Cl_2/hexanes 1:1, gradient to pure CH_2Cl_2) to provide **10^{Ph}Pd** (∼55% yield, 12−13 mg). **10^{Ph}Pd**: MW = 781.22 g/mol; R_f = 0.48 (silica−CH_2Cl_2). ^{1}H NMR (400 MHz, $CDCl_3$, 300 K): δ 8.43 (d, J = 4.0 Hz, 2H), 8.427 (s, 2H), 8.18 (d, J = 4.9 Hz, 2H), 8.05−8.01 (m, 6H), 7.75 (d, J = 6.5 Hz, 2H), 7.70−7.66 (m, 8H), 7.62−7.59 (m, 4H), 5.99 (s, 2H), 2.99 (s, 6H). ^{13}C NMR (100 MHz, $CDCl_3$, 300 K): δ 146.9, 145.4, 141.3, 141.2, 139.7, 137.9, 133.9, 133.4, 132.8, 132.2, 131.6, 131.1, 129.1, 128.2, 127.8, 127.34, 127.3, 127.2, 127.1, 126.84, 126.81, 125.5, 114.8, 81.3, 57.8. UV−vis [CH_2Cl_2; λ_{max}, nm (log ε, M^{-1} cm^{-1})]: 410 (5.25), 495 (3.75), 561 (3.97), 593 (4.66). HR-MS (ESI$^+$, 100% CH_3CN, TOF). Calcd for $C_{46}H_{35}N_4O_2Pd$ ([M + H]$^+$): m/z 781.1789. Found: m/z 781.1819.

*meso-Tetrakis[4-(trifluoromethyl)phenyl]-2,3-cis-dimethoxychlorin (**$10^{CF_3}H_2$**).* To a solution of *meso*-tetrakis[4-(trifluoromethyl)-phenyl]-2,3-*cis*-dihydroxychlorin (**$8^{CF_3}H_2$**; 150 mg, 1.63×10^{-4} mol) in tetrahydrofuran (25 mL) was added a molar excess of NaH (∼75 mg, 60% emulsion in oil) in portions and under a dry N_2 atmosphere. After the reaction mixture was stirred for 30−45 min at ambient conditions, CH_3I (0.020 mL, 3.26×10^{-4} mol) was added with a glass syringe (***Caution!** Gloves and fume hood!*), and the mixture was stirred for 2 h at ambient temperature. After the starting material was consumed (reaction monitored by TLC), the reaction was quenched by the slow addition of water and the product was extracted into CH_2Cl_2 (25 mL). The organic layer was washed with water (3 × 10 mL), dried (Na_2SO_4), filtered, and evaporated to dryness by rotary evaporation. The residue was purified by column chromatography (silica−CH_2Cl_2 1:1, gradient to pure CH_2Cl_2) to provide **$10^{CF_3}H_2$**, after recrystallization by the slow solvent exchange of CH_2Cl_2 to MeOH on the rotary evaporator, as a red-brown crystalline material (50−60% yield, 77−93 mg). **$10^{CF_3}H_2$**: MW = 948.81 g/mol; R_f = 0.65 (silica−CH_2Cl_2). ^{1}H NMR (400 MHz, $CDCl_3$, 300 K): δ 8.63 (d, J = 4.9 Hz, 2H), 8.45 (s, 2H), 8.33 (d, J = 4.7 Hz, 2H), 8.27−8.26 (m, 4H), 8.21 (d, J = 7.5 Hz, 2H), 8.04−7.93 (m, 10H), 5.97 (s, 2H), 3.01 (s, 6H), −1.96 (s, 2H). ^{13}C NMR (100 MHz, $CDCl_3$, 300 K): δ 160.2, 152.8, 145.2, 140.2, 135.4, 134.4, 134.2, 134.0, 132.9, 131.6, 130.4, 130.1, 129.8, 128.1, 125.8, 124.8, 124.3, 124.1, 123.85, 123.82, 123.1, 121.5, 113.0, 81.6, 58.4. UV−vis [CH_2Cl_2; λ_{max}, nm (log ε, M^{-1} cm^{-1})]: 414 (5.31), 515 (4.19), 543 (4.12), 592 (3.85), 645 (4.46). HR-MS (ESI$^+$, 100% CH_3CN, TOF). Calcd for $C_{50}H_{33}F_{12}N_4O_2$ ([M + H]$^+$): m/z 949.2406. Found: m/z 949.2394.

*[meso-Tetrakis[4-(trifluoromethyl)phenyl]-2,3-cis-dimethoxychlorinato]nickel(II) (**10^{CF_3}Ni**).* To a solution of **$10^{CF_3}H_2$** (15.0 mg, 1.58×10^{-5} mol) in C_6H_5CN (10 mL) was added 2−3 equiv of $Ni(OAc)_2·4H_2O$ (12.0 mg, 4.74×10^{-5} mol). The reaction mixture was refluxed for 15−20 min. After the starting material was consumed (TLC control), the reaction mixture was evaporated to dryness by rotary evaporation. The residue was dissolved in CH_2Cl_2 (15 mL) and washed with water (3 × 10 mL), and the organic layer was dried (Na_2SO_4), filtered, and evaporated to dryness by rotary evaporation. The crude product was purified by column chromatography (silica−CH_2Cl_2/hexanes 1:1, gradient to pure CH_2Cl_2) to provide **10^{CF_3}Ni** (∼60% yield, 9−10 mg). **10^{CF_3}Ni**: MW = 1005.49 g/mol; R_f = 0.83 (silica−CH_2Cl_2/hexanes 1:1). ^{1}H NMR (400 MHz, $CDCl_3$, 300 K): δ 8.29 (d, J = 5.0 Hz, 2H), 8.14 (s, 2H), 8.09 (d, J = 4.9 Hz, 2H), 7.99−7.97 (m, 4H), 7.91−7.89 (m, 4H), 7.82 (q, J = 7.5 Hz, 8H), 5.46 (s, 2H), 2.98 (s, 6H). ^{13}C NMR (100 MHz, $CDCl_3$, 300 K): δ 146.1, 145.4, 143.4, 143.2, 141.1, 138.3, 133.2, 133.0, 132.4, 132.2, 130.5, 130.2, 129.9, 129.6, 129.17, 129.11, 127.7, 125.7, 124.3, 124.2, 123.0, 122.7, 110.8, 83.6, 58.1. UV−vis [CH_2Cl_2; λ_{max}, nm (log ε, M^{-1} cm^{-1})]: 416 (5.10), 571 (sh), 614 (4.28). HR-MS (ESI$^+$, 100% CH_3CN, TOF). Calcd for $C_{50}H_{31}F_{12}N_4NiO_2$ ([M + H]$^+$): m/z 1005.1603. Found: m/z 1005.1609.

*[meso-Tetrakis[4-(trifluoromethyl)phenyl]-2,3-cis-dimethoxychlorinato]zinc(II) (**10^{CF_3}Zn**).* To a solution of dimethoxychlorin **$10^{CF_3}H_2$** (11.0 mg, 1.16×10^{-5} mol) in $CHCl_3$ (7.0 mL) was added a solution of $Zn(OAc)_2·2H_2O$ (20.0 mg, 9.27×10^{-5} mol) in MeOH (1.0 mL). The reaction mixture was heated to reflux for 1.5−2 h. After the starting material was consumed (monitored by TLC), the reaction mixture was evaporated to dryness by rotary evaporation, the residue was dissolved in CH_2Cl_2 (10 mL) and washed with water (3 × 10 mL), and the organic layer was dried (Na_2SO_4), filtered, and evaporated to dryness by rotary evaporation. The residue was purified by column chromatography (silica−CH_2Cl_2/hexanes 1:1, gradient to pure CH_2Cl_2) to provide **10^{CF_3}Zn** (95% yield, 11.0 mg). **10^{CF_3}Zn**: MW = 1012.1768 g/mol; R_f = 0.38 (silica−2% MeOH in CH_2Cl_2). ^{1}H NMR (400 MHz, $CDCl_3$, 300 K): δ 8.50 (d, J = 4.8 Hz, 2H), 8.38 (s, 2H), 8.20 (d, J = 7.6 Hz, 2H), 8.20 (br s, 4H), 8.14 (d, J = 4.8 Hz, 2H), 7.98−7.88 (m, 10H), 5.80 (s, 2H), 3.04 (s, 6H). ^{13}C NMR (100 MHz, $CDCl_3$, 300 K): δ 156.3, 154.3, 148.1, 146.5, 142.33, 142.27, 134.1, 133.59, 133.54, 132.6, 131.3, 129.5, 128.5, 127.8, 127.5, 127.04, 127.01, 126.9, 126.62, 126.59, 125.1, 114.2, 81.0, 58.4. UV−vis [CH_2Cl_2; λ_{max}, nm (log ε, M^{-1} cm^{-1})]: 415 (5.35), 581 (3.87), 614 (4.46). HR-MS (ESI$^+$, 100% CH_3CN, TOF). Calcd for $C_{50}H_{31}F_{12}N_4O_2Zn$ ([M + H]$^+$): m/z 1011.1541. Found: m/z 1011.1502.

*[meso-Tetrakis[4-(trifluoromethyl)phenyl]-2,3-cis-dimethoxychlorinato]palladium(II) (**10^{CF_3}Pd**).* To a solution of dimethoxychlorin **$10^{CF_3}H_2$** (20.0 mg, 2.10×10^{-5} mol) in C_6H_5CN (10 mL) was added $Pd(OAc)_2$ (19.0 mg, 8.43×10^{-5} mol). The reaction mixture was refluxed for 2−3 h. After the starting material was consumed (monitored by TLC), the reaction mixture was evaporated to dryness by rotary evaporation. The residue was dissolved in CH_2Cl_2 (15 mL) and washed with water (3 × 10 mL). The organic layer was dried (Na_2SO_4), filtered, and evaporated to dryness by rotary evaporation. The crude product was purified by column chromatography (silica−CH_2Cl_2/hexanes 1:1, gradient to pure CH_2Cl_2) to provide **10^{CF_3}Pd** (∼60% yield, 13−14 mg). **10^{CF_3}Pd**: MW = 1053.22 g/mol; R_f = 0.36 (silica−CH_2Cl_2/hexanes 1:1). ^{1}H NMR (400 MHz, $CDCl_3$, 300 K): δ 8.38 (d, J = 6.4 Hz, 2H), 8.37 (s, 2H), 8.17−8.12 (m, 8H), 7.98−7.94 (m, 6H), 7.89 (br s, 4H), 5.91 (s, 2H), 2.99 (s, 6H). ^{13}C NMR (100 MHz, $CDCl_3$, 300 K): δ 146.9, 145.1, 144.6, 139.3, 137.7, 134.0, 133.4, 132.2, 131.8, 131.3, 130.6, 130.2, 130.0, 129.7, 129.1, 128.7, 128.5, 127.6, 125.8, 124.3, 124.0, 123.1, 113.8, 81.1, 57.8. UV−vis [CH_2Cl_2; λ_{max}, nm (log ε, M^{-1} cm^{-1})]: 409

DOI: 10.1021/acs.inorgchem.7b00799
Inorg. Chem. 2017, 56, 11490−11502

(5.26), 494 (3.83), 560 (3.97), 594 (4.69). HR-MS (ESI$^+$, 100% CH_3CN, TOF). Calcd for $C_{50}H_{31}F_{12}N_4O_2Pd$ ([M + H]$^+$): m/z 1053.1285. Found: m/z 1053.1308.

*[meso-Tetrakis[4-(trifluoromethyl)phenyl]-2,3-cis-dimethoxychlorinato]silver(II) (**10^{CF_3}Ag**).* To a solution of dimethoxychlorin **10^{CF_3}H$_2$** (16.0 mg, 1.70×10^{-5} mol) in C_6H_5CN (5 mL) was added AgOAc (10 mg, 5.90×10^{-5} mol). The reaction mixture was refluxed for 30 min. After the starting material was consumed (monitored by TLC), the reaction mixture was evaporated to dryness by rotary evaporation. The crude product was purified by column chromatography (silica–CH_2Cl_2/hexanes 1:1, gradient to pure CH_2Cl_2) to provide **10^{CF_3}Ag** (~62% yield, 11 mg). **10^{CF_3}Ag**: MW = 1054.67 g/mol; R_f = 0.32 (silica–CH_2Cl_2/hexanes 1:1). UV–vis [CH_2Cl_2; λ_{max}, nm (log ε, M^{-1} cm^{-1})]: 420 (5.31), 583 (sh), 601 (4.32). HR-MS (ESI$^+$, 100% CH_3CN, TOF). Calcd for $C_{50}H_{30}AgF_{12}N_4O_2$ (M^+): m/z 1053.1223. Found: m/z 1053.1255.

*meso-Tetrakis[4-(trifluoromethyl)phenyl]-2,3-trans-diethoxymorpholine (**11^{CF_3}H$_2$**).* To a solution of *meso*-tetrakis[4-(trifluoromethyl)-phenyl]-2,3-*cis*-dihydroxychlorin (**9^{CF_3}H$_2$**; 100 mg, 1.09×10^{-4} mol) in $CHCl_3$ (20 mL) and ethanol (EtOH; 1–2 mL) was added silica gel-supported $NaIO_4$ (~1.0 g)[36] under a N_2 atmosphere, and the mixture was stirred overnight at ambient temperature. After the starting material was consumed (monitored by TLC), the mixture was filtered (glass frit M) and the filter cake washed with $CHCl_3$. The filtrate was evaporated to dryness by rotary evaporation. The crude product was purified by column chromatography (silica–CH_2Cl_2/hexanes 1:1, gradient to pure CH_2Cl_2) to provide **11^{CF_3}H$_2$**, after recrystallization by the slow solvent exchange of $CHCl_3$ to EtOH on a rotary evaporator, as a red-brown crystalline material (70–80% yield, 75–85 mg). **11^{CF_3}H$_2$**: MW = 992.87 g/mol; R_f = 0.45 (silica–CH_2Cl_2/hexanes 1:1). ^{1}H NMR (400 MHz, $CDCl_3$, 300 K): δ 8.67 (d, J = 7.6 Hz, 2H), 8.47 (d, J = 5.0 Hz, 2H), 8.31 (s, 2H), 8.10 (br s, 2H), 8.10 (d, J = 5.2 Hz, 2H), 7.98 (br s, 8H), 7.77 (d, J = 8 Hz, 2H), 7.41 (d, J = 7.6, 2H), 6.41 (s, 2H), 3.64–3.57 (m, 2H), 3.27–3.19 (m, 2H), 0.92 (t, J = 7.1 Hz, 6H), −0.93 (s, 2H). ^{13}C NMR (100 MHz, $CDCl_3$, 300 K): δ 151.7, 146.8, 144.2, 143.7, 138.6, 134.3, 133.2, 132.9, 131.7, 130.8, 129.8, 129.5, 129.1, 128.8, 127.0, 124.9, 124.7, 123.7, 123.3, 123.0, 122.0, 120.8, 112.6, 93.6, 62.5, 14.0. UV–vis [CH_2Cl_2; λ_{max}, nm (log ε, M^{-1} cm^{-1})]: 418 (5.11), 526 (3.98), 559 (3.87), 617 (3.61), 676 (4.08). HR-MS (ESI$^+$, 100% CH_3CN, TOF). Calcd for $C_{52}H_{37}F_{12}N_4O_3$ ([M + H]$^+$): m/z 993.2669. Found: m/z 993.2647.

*[meso-Tetrakis[4-(trifluoromethyl)phenyl]-2,3-trans-diethoxymorpholinochlorinato]copper(II) (**11^{CF_3}Cu**).* To a solution of diethoxymorpholine **11^{CF_3}H$_2$** (20.0 mg, 2.01×10^{-5} mol) in $CHCl_3$ (5 mL) was added a solution of $Cu(OAc)_2 \cdot H_2O$ (30.0 mg, 1.51×10^{-4} mol) in EtOH (3–4 mL). The reaction mixture was heated to reflux overnight. After the starting material was consumed (monitored by TLC), the reaction mixture was evaporated to dryness by rotary evaporation. The crude product was purified by column chromatography (silica–CH_2Cl_2/hexanes 1:1, gradient to pure CH_2Cl_2) to provide **11^{CF_3}Cu** (~90% yield, 19 mg). **11^{CF_3}Cu**: MW = 1054.40 g/mol; R_f = 0.64 (silica–CH_2Cl_2/hexanes 1:1). UV–vis [CH_2Cl_2; λ_{max}, nm (log ε, M^{-1} cm^{-1})]: 421 (5.18), 599 (sh), 644 (4.13). HR-MS (ESI$^+$, 100% CH_3CN, TOF). Calcd for $C_{52}H_{34}CuF_{12}N_4O_3$ (M^+): m/z 1053.1730. Found: m/z 1053.1713.

*[meso-Tetrakis[4-(trifluoromethyl)phenyl]-2,3-trans-diethoxymorpholinochlorinato]zinc(II) (**11^{CF_3}Zn**).* To a solution of diethoxymorpholine **11^{CF_3}H$_2$** (12.0 mg, 1.21×10^{-5} mol) in $CHCl_3$ (7 mL) was added a solution of $Zn(OAc)_2 \cdot 2H_2O$ (11.0 mg, 4.83×10^{-5} mol) in EtOH (1.0 mL). The reaction mixture was heated to reflux for 1 h. After the starting material was consumed (monitored by TLC), the reaction mixture was evaporated to dryness by rotary evaporation. The crude product was purified by preparative TLC (20 × 20 cm, 500 μm, silica–CH_2Cl_2/hexanes 1:1) to provide **11^{CF_3}Zn** (~55% yield, ~7 mg). The product was difficult to purify because it degraded slowly on the preparative TLC plate. **11^{CF_3}Zn**: MW = 1056.23 g/mol; R_f = 0.49 (silica–CH_2Cl_2). ^{1}H NMR (400 MHz, $CDCl_3$, 300 K): δ 8.58 (d, J = 8.0 Hz, 2H), 8.37 (d, J = 4.4 Hz, 2H), 8.34 (br s, 2H), 8.22 (s, 2H), 8.06 (d, J = 7.6 Hz, 2H), 7.99 (br s, 2H), 7.91 (d, J = 4.8 Hz, 2H), 7.89 (br s, 4H), 7.73 (d, J = 7.6 Hz, 2H), 7.35 (d, J = 8.0 Hz, 2H), 6.27 (s, 2H), 3.75–3.68 (m, 2H), 3.33–3.25 (m, 2H), 0.92 (t, J = 7.2 Hz, 6H). ^{13}C NMR (100 MHz, $CDCl_3$, 300 K): δ 153.1, 146.8, 145.7, 144.3, 144.2, 144.0, 132.7, 132.4, 132.3, 132.28, 132.0, 130.7, 129.4, 129.1, 128.7, 128.4, 127.3, 124.6, 123.3, 122.9, 122.6, 121.9, 111.8, 94.0, 62.3, 13.8. UV–vis [CH_2Cl_2; λ_{max}, nm (Rel. I)]: 427 (1.00), 602 (0.05), 642 (0.14). HR-MS (ESI$^+$, 100% CH_3CN, TOF). Calcd for $C_{52}H_{34}F_{12}N_4O_3Zn$ (M^+): m/z 1054.1725. Found: m/z 1054.1709.

*[meso-Tetrakis[4-(trifluoromethyl)phenyl]-2,3-trans-diethoxymorpholinochlorinato]palladium(II) (**11^{CF_3}Pd**).* To a solution of diethoxymorpholine **11^{CF_3}H$_2$** (15.0 mg, 1.5×10^{-5} mol) in pyridine (5 mL) was added $Pd(OAc)_2$ (15.0 mg, 6.68×10^{-5} mol). The reaction mixture was heated to reflux overnight. After the starting material was consumed (monitored by TLC), the reaction mixture was evaporated to dryness by rotary evaporation. The residue was dissolved in CH_2Cl_2 (15 mL) and washed with water (3 × 10 mL). The organic layer was dried (Na_2SO_4), filtered, and evaporated to dryness by rotary evaporation. The crude product was purified by column chromatography (silica–CH_2Cl_2/hexanes 1:1, gradient to pure CH_2Cl_2) to provide **11^{CF_3}Pd** (~90% yield, 15 mg). **11^{CF_3}Pd**: MW = 1097.27 g/mol; R_f = 0.62 (silica–CH_2Cl_2/hexanes 1:1). ^{1}H NMR (400 MHz, $CDCl_3$, 300 K): δ 8.60 (d, J = 8.0 Hz, 2H), 8.41 (d, J = 6.0 Hz, 2H), 8.27 (d, J = 5.2 Hz, 2H), 8.26 (s, 2H), 8.07 (dd, J = 8.0 and 1.2 Hz, 2H), 8.02 (d, J = 6.4 Hz, 2H), 7.94 (d, J = 5.2 Hz, 2H), 7.87 (d, J = 5.6 Hz, 2H), 7.79 (d, J = 6.0 Hz, 2H), 7.73 (d, J = 7.6 Hz, 2H), 7.28 (d J = 8.0 Hz, 2H), 6.32 (s, 2H), 3.65–3.57 (m, 2H), 3.19–3.11 (m, 2H), 0.81 (t, J = 7.1 Hz, 6H). ^{13}C NMR (100 MHz, $CDCl_3$, 300 K): δ 144.7, 144.0, 143.7, 140.1, 140.0, 138.0, 133.5, 133.4, 132.3, 132.0, 130.6, 130.3, 130.0, 129.7, 128.6, 126.0, 125.8, 124.7, 124.4, 124.0, 123.2, 113.4, 96.0, 63.2, 14.7. UV–vis [CH_2Cl_2; λ_{max}, nm (log ε, M^{-1} cm^{-1})]: 424 (5.33), 583 (sh), 620 (4.82). HR-MS (ESI$^+$, 100% CH_3CN, TOF). Calcd for $C_{52}H_{34}F_{12}N_4O_3Pd$ (M^+): m/z 1096.1469. Found: m/z 1096.1476.

*[meso-Tetrakis[4-(trifluoromethyl)phenyl]-2,3-trans-diethoxymorpholinochlorinato]silver(II) (**11^{CF_3}Ag**).* To a solution of diethoxymorpholine **11^{CF_3}H$_2$** (20.0 mg, 2.01×10^{-5} mol) in pyridine (10 mL) was added a solution of AgOAc (15.0 mg, 9.05×10^{-5} mol) in MeOH (3–4 mL). The reaction mixture was heated to reflux overnight. After the starting material was consumed (monitored by TLC), the reaction mixture was evaporated to dryness by rotary evaporation. The crude product was purified by column chromatography (silica–CH_2Cl_2/hexanes 1:1, gradient to pure CH_2Cl_2) to provide **11^{CF_3}Ag** (~63% yield, 14 mg). **11^{CF_3}Ag**: MW = 1098.72 g/mol; R_f = 0.60 (silica–CH_2Cl_2/hexanes 1:1). UV–vis [CH_2Cl_2; λ_{max}, nm (log ε, M^{-1} cm^{-1})]: 425 (4.87), 587 (sh), 604 (3.95). HR-MS (ESI$^+$, 100% CH_3CN, TOF). Calcd for $C_{52}H_{34}AgF_{12}N_4O_3$ (M^+): m/z 1097.1485. Found: m/z 1097.1500.

X-ray Diffractometry. *Single-Crystal X-ray Diffraction.* Data were collected using a Bruker Apex II CCD or a Quest CMOS diffractometer with Mo Kα radiation (λ = 0.71073 Å). The instruments feature fine-focus sealed tube X-ray sources with plane or curved graphite monochromators. Single crystals were mounted on Mitegen micromesh mounts using a trace of mineral oil and cooled in situ to 100(2) K for data collection. Frames were collected, reflections were indexed and processed, and the files were scaled and corrected for absorption using *Apex2* or *Apex3*. The space groups were assigned, and the structures were solved by direct methods using *XPREP* within the *SHELXTL* suite of programs and refined by full-matrix least-squares against F^2 with all reflections using *SHELXL2016* with the graphical interface *SHELXLE*.[37] If not specified otherwise, H atoms attached to C and N atoms and hydroxyl H atoms were positioned geometrically and constrained to ride on their parent atoms, with C–H bond distances of 0.95 Å for alkene and aromatic C–H moieties, 1.00, 0.99, and 0.98 Å for aliphatic C–H, CH_2, and CH_3 moieties, and 0.88 Å for the N–H moiety, respectively. Methyl H atoms were allowed to rotate but not to tip to best fit the experimental electron density. U_{iso}(H) values were set to a multiple of U_{eq}(C/N) with 1.5 for CH_3 and 1.2 for C–H, CH_2, and N–H units, respectively.

Disorder has been observed in several of the described crystal structures. A detailed description is available in the Supporting Information. We detail here the models used for disorders involving the pyrrole/pyrroline/morpholine moieties, but not if only their substituents were involved, only involving the *meso*-aryl groups or solvent.

DOI: 10.1021/acs.inorgchem.7b00799
Inorg. Chem. 2017, 56, 11490–11502

Table 1. Crystal Data and Refinement Details for the Compounds Indicated[a]

	$10^{CF_3}Ni$	$10^{CF_3}Pd$	$10^{CF_3}Zn$	$10^{Ph}Cu$
chemical formula	$C_{50}H_{30}F_{12}N_4NiO_2$	$C_{53}H_{37}F_{12}N_4O_2Pd$	$C_{55}H_{35}F_{12}N_5O_2Zn$	$C_{46}H_{34}CuN_4O_2$
M_r	1005.49	1096.30	1091.25	738.31
cryst syst, space group	orthorhombic, *Pbca*	triclinic, $P\bar{1}$	triclinic, $P\bar{1}$	monoclinic, $P2_1/c$
a, *b*, *c* (Å)	22.399(3), 15.8523(19), 23.089(3)	10.8998(3), 14.9401(5), 15.7540(5)	11.5956(6), 14.9797(7), 15.6698(8)	14.761(3), 9.5806(17), 25.103(4)
α, β, γ (deg)	90, 90, 90	67.8972(19), 84.489(2), 72.3069(18)	110.543(3), 93.266(3), 110.166(3)	90, 99.330(3), 90
V (Å^3)	8198.3(18)	2263.99(13)	2343.0(2)	3503.2(11)
Z	8	2	2	4
D_x (Mg/m^3)	1.629	1.608	1.547	1.400
μ (mm^{-1})	0.58	0.51	0.62	0.67
$R[F^2 > 2\sigma(F^2)]$, $wR(F^2)$[b]	0.063, 0.184	0.058, 0.139	0.070, 0.217	0.059, 0.130
	$w = 1/[\sigma^2(F_0^2) + (0.090P)^2 + 17.8173P]$	$w = 1/[\sigma^2(F_0^2) + (0.0257P)^2 + 6.8374P]$	$w = 1/[\sigma^2(F_0^2) + (0.135P)^2]$	$w = 1/[\sigma^2(F_0^2) + (0.0363P)^2 + 5.1073P]$
CCDC	1538285	1538284	1538290	1538288
	$11^{CF_3}Ag$	$11^{CF_3}Cu$	$11^{CF_3}Pd$	$11^{CF_3}Zn$
chemical formula	$C_{52}H_{34}AgF_{12}N_4O_3$	$C_{52}H_{34}CuF_{12}N_4O_3$	$C_{52}H_{34}F_{12}N_4O_3Pd$	$C_{57}H_{39}F_{12}N_5O_3Zn$
M_r	1098.70	1054.37	1097.23	1135.30
cryst syst, space group	triclinic, $P\bar{1}$	triclinic, $P\bar{1}$	triclinic, $P\bar{1}$	triclinic, $P\bar{1}$
a, *b*, *c* (Å)	13.441(4), 14.166(4), 14.712(4)	13.435(3), 13.603(3), 14.869(4)	13.534(3), 13.996(2), 14.719(3)	12.380(4), 13.946(4), 15.787(5)
α, β, γ (deg)	114.136(5), 101.755(4), 108.556(4)	113.941(3), 99.729(3), 108.126(3)	113.944(2), 100.727(4), 109.081(3)	79.360(5), 71.592(5), 72.439(5)
V (Å^3)	2235.7(10)	2219.8(9)	2238.1(7)	2453.6(13)
Z	2	2	2	2
D_x (Mg/m^3)	1.632	1.577	1.628	1.537
μ (mm^{-1})	0.55	0.59	0.52	0.60
$R[F^2 > 2\sigma(F^2)]$, $wR(F^2)$	0.064, 0.169	0.067, 0.139	0.036, 0.089	0.086, 0.200
	$w = 1/[\sigma^2(F_0^2) + (0.0493P)^2 + 7.5298P]$	$w = 1/[\sigma^2(F_0^2) + (0.0332P)^2]$	$w = 1/[\sigma^2(F_0^2) + (0.0403P)^2 + 1.4037P]$	$w = 1/[\sigma^2(F_0^2) + (0.0399P)^2 + 8.689P]$
CCDC	1538289	1538283	1538287	1538286

[a]Experiments were carried out at 100 K with Mo Kα radiation. H atom parameters were constrained. [b]$P = (F_0^2 + 2F_c^2)/3$.

For $\mathbf{10^{CF_3}Pd}$, the dimethoxy-substituted pyrroline is 1:1 disordered over two alternative positions and disordered with a pyrrole moiety each. The disorder is induced by the methoxy groups of one of the sites overlapping with their symmetry-equivalent counterparts of a neighboring molecule across an inversion center. The disorder induces also 1:1 disorder for three of the four (trifluoromethyl)phenylene substituents and for a solvate hexane molecule neighboring the second dimethoxy unit. The hexane molecule is shifted as a response to the presence or absence of the methoxy groups and is 1:1 disordered across an inversion center. Equivalent bond distances in the disordered pyrrole and pyrroline were restrained to be similar and, for the pyrrole, to be similar to a nondisordered pyrrole. All *p*-(trifluoromethyl)phenyl substituents were restrained to have similar geometries. The *ipso*-C atoms were excluded from the disorder model for two of the three disordered substituents. The C−C bond distances of the hexane molecule were restrained to target distances [1.53(2) and 1.50(2) Å respectively]. For all disordered atoms, the U^{ij} components of atomic displacement parameters (ADPs) were restrained to be similar for atoms closer to each other than 1.7 Å.

For $\mathbf{11^{CF_3}Ag}$, the structure shows disorder of the morpholine moiety and of three of the CF_3 groups. Equivalent moieties and some equivalent bond distances in the disordered regions were each restrained to be similar, and the U^{ij} components of ADPs were restrained to be similar for atoms closer to each other than 1.7 Å. F7B−F9B were restrained to be close to isotropic. The occupancy rates for the major moieties were refined to 0.838(4), 0.622(14), 0.761(7), and 0.592(11).

For $\mathbf{11^{CF_3}Zn}$, large parts of the structure are disordered by the pseudomirror symmetry of the morpholino moiety. The disorder extends out to two of the *p*-(trifluoromethyl)phenyl groups. The two disordered units were restrained to have similar geometries, and equivalent overlapping atoms were constrained to have identical ADPs. The occupancy ratio for the two moieties refined to 0.679(2):0.321(2). The U^{ij} components of ADPs of disordered atoms were restrained to be similar for atoms closer to each other than 1.7 Å

Crystal data and refinement details are given in Table 1 and in more detail in the Supporting Information. Complete crystallographic data, in CIF format, have been deposited with the Cambridge Crystallographic Data Centre. CCDC 1538283−1538290 contain the supplementary crystallographic data for this paper. These data can be obtained free of charge from The Cambridge Crystallographic Data Centre via www.ccdc.cam.ac.uk/data_request/cif.

■ ASSOCIATED CONTENT

Supporting Information

The Supporting Information is available free of charge on the ACS Publications website at DOI: 10.1021/acs.inorgchem.7b00799.

Reproduction of the experimental data (such as ^{1}H and ^{13}C NMR and MS spectra) of all new compounds obtained (PDF)

Accession Codes

CCDC 1538283−1538290 contain the supplementary crystallographic data for this paper. These data can be obtained free of charge via www.ccdc.cam.ac.uk/data_request/cif, or by emailing data_request@ccdc.cam.ac.uk, or by contacting The Cambridge Crystallographic Data Centre, 12 Union Road, Cambridge CB2 1EZ, UK; fax: +44 1223 336033.

DOI: 10.1021/acs.inorgchem.7b00799
Inorg. Chem. 2017, 56, 11490−11502

AUTHOR INFORMATION

Corresponding Author

*E-mail: c.bruckner@uconn.edu. Tel: (+1) 860 486-2743. Fax: (+1) 860 486-2981.

ORCID

Christian Brückner: 0000-0002-1560-7345

Present Addresses

‡A.L.T.: Department of Physiology and Biophysics, University of Illinois at Chicago, 835 South Wolcott Street, Chicago, IL 60612-7342.

⊥L.S.: Department of Chemistry and Biochemistry, Old Dominion University, 110 Alfriend Chemistry Building, Norfolk, VA 23529-0126.

¶M.Z.: Department of Chemistry, Purdue University, 560 Oval Drive, West Lafayette, IN 47907-2084.

Author Contributions

§Equal contributions.

Notes

The authors declare no competing financial interest.

ACKNOWLEDGMENTS

This material is based upon work supported by the National Science Foundation through Grants CHE-1058846 and CHE-1465133 (to C.B.), an REU Fellowship through Grant CHE-1062946 (to A.L.T.), the Major Research Instrumentation Programs CHE-1625543 (Purdue) and DMR-1337296 (Youngstown State), the Ohio Board of Regents (Grant CAP-491), and Youngstown State University.

REFERENCES

(1) Taniguchi, M.; Lindsey, J. S. Synthetic Chlorins, Possible Surrogates for Chlorophylls, Prepared by Derivatization of Porphyrins. *Chem. Rev.* **2017**, *117*, 344−535.

(2) (a) Suslick, K. S. Shape-Selective Oxidation by Metalloporphyrins. In *The Porphyrin Handbook*; Kadish, K. M., Smith, K. M., Guilard, R., Eds.; Academic Press: San Diego, 2000; Vol. *4*, pp 41−63. (b) Meunier, B.; Robert, A.; Pratviel, G.; Bernadou, J. Metalloporphyrins in Catalytic Oxidations and Oxidative DNA Cleavage. In *The Porphyrin Handbook*; Kadish, K. M., Smith, K. M., Guilard, R., Eds.; Academic Press: San Diego, 2000; Vol. *4*, pp 119−187. (c) Ruppel, J. V.; Fields, K. B.; Snyder, N. L.; Zhang, X. P. Metalloporphyrin-Catalyzed Asymmetric Atom/Group Transfer Reactions. In *Handbook of Porphyrin Science*; Kadish, K. M., Smith, K. M., Guilard, R., Eds.; World Scientific: Hackensack, NJ, 2010; Vol. *10*, pp 1−182.

(3) Jurow, M.; Schuckman, A. E.; Batteas, J. D.; Drain, C. M. Porphyrins as Molecular Electronic Components of Functional Devices. *Coord. Chem. Rev.* **2010**, *254*, 2297−2310.

(4) (a) Grätzel, M. Dye-Sensitized Solar Cells. *J. Photochem. Photobiol., C* **2003**, *4*, 145−153. (b) Lindsey, J. S.; Mass, O.; Chen, C.-Y. Tapping the near-Infrared Spectral Region with Bacteriochlorin Arrays. *New J. Chem.* **2011**, *35*, 511−516. (c) Lindsey, J. S. *De novo* Synthesis of *Gem*-Dialkyl Chlorophyll Analogues for Probing and Emulating Our Green World. *Chem. Rev.* **2015**, *115*, 6534−6620.

(5) (a) Sternberg, E. D.; Dolphin, D.; Brückner, C. Porphyrin-Based Photosensitizers for Use in Photodynamic Therapy. *Tetrahedron* **1998**, *54*, 4151−4202. (b) Ethirajan, M.; Chen, Y.; Joshi, P.; Pandey, R. K. The Role of Porphyrin Chemistry in Tumor Imaging and Photodynamic Therapy. *Chem. Soc. Rev.* **2011**, *40*, 340−362.

(6) de Haas, R. R.; van Gijlswijk, R. P. M.; van der Tol, E. B.; Zijlmans, H. J. M. A. A.; Bakker-Schut, T.; Bonnet, J.; Verwoerd, N. P.; Tanke, H. J. Platinum Porphyrins as Phosphorescent Label for Time-Resolved Microscopy. *J. Histochem. Cytochem.* **1997**, *45*, 1279−1292.

(7) (a) Schäferling, M. The Art of Fluorescence Imaging with Chemical Sensors. *Angew. Chem., Int. Ed.* **2012**, *51*, 3532−3554. (b) Huang, H.; Song, W.; Rieffel, J.; Lovell, J. F. Emerging Applications of Porphyrins in Photomedicine. *Front. Phys.* **2015**, *3*, XXX.

(8) (a) Fouchet, J.; Jeandon, C.; Ruppert, R.; Callot, H. J. Locked π-Expanded Chlorins in Two Steps from Simple Tetraarylporphyrins. *Org. Lett.* **2005**, *7*, 5257−5260. (b) Fox, S.; Boyle, R. W. Synthetic Routes to Porphyrins Bearing Fused Rings. *Tetrahedron* **2006**, *62*, 10039−10054. (c) Davis, N. K. S.; Thompson, A. L.; Anderson, H. L. A Porphyrin Fused to Four Anthracenes. *J. Am. Chem. Soc.* **2011**, *133*, 30−31. (d) Akhigbe, J.; Luciano, M.; Zeller, M.; Brückner, C. Mono- and Bisquinoline-Annulated Porphyrins from Porphyrin *β,β′*-Dione Oximes. *J. Org. Chem.* **2015**, *80*, 499−511. (e) Hyland, M. A.; Hewage, N.; Panther, K.; Nimthong Roldan, A.; Zeller, M.; Samaraweera, M.; Gascón, J. A.; Brückner, C. Chromene-Annulated Bacteriochlorins. *J. Org. Chem.* **2016**, *81*, 3603−3618.

(9) (a) Spellane, P. J.; Gouterman, M.; Antipas, A.; Kim, S.; Liu, Y. C. Electronic Spectra and Four-Orbital Energies of Free-Base, Zinc, Copper, and Palladium Tetrakis(perfluorophenyl)porphyrins. *Inorg. Chem.* **1980**, *19*, 386−391. (b) Ojadi, E. C. A.; Linschitz, H.; Gouterman, M.; Walter, R. I.; Lindsey, J. S.; Wagner, R. W.; Droupadi, P. R.; Wang, W. Sequential Protonation of *meso*-[*p*-(Dimethylamino)phenyl]porphyrins: Charge-Transfer Excited States Producing Hyperporphyrins. *J. Phys. Chem.* **1993**, *97*, 13192−13197. (c) Brückner, C.; Foss, P. C. D.; Sullivan, J. O.; Pelto, R.; Zeller, M.; Birge, R. R.; Crundwell, G. Origin of the Bathochromically Shifted Optical Spectra of *meso*-Tetrakis-2- and 3-Thienylporphyrins as Compared to *meso*-Tetrakisphenylporphyrin. *Phys. Chem. Chem. Phys.* **2006**, *8*, 2402−2412.

(10) Senge, M. O. Exercises in Molecular Gymnastics-Bending, Stretching and Twisting Porphyrins. *Chem. Commun.* **2006**, 243−256.

(11) Brückner, C.; Samankumara, L.; Ogikubo, J. Syntheses of Bacteriochlorins and Isobacteriochlorins. In *Handbook of Porphyrin Science*; Kadish, K. M., Smith, K. M., Guilard, R., Eds.; World Scientific: River Edge, NY, 2012; Vol. *17*, pp 1−112.

(12) (a) Shelnutt, J. A.; Song, X.-Z.; Ma, J.-G.; Jia, S.-L.; Jentzen, W.; Medforth, C. J. Nonplanar Porphyrins and Their Significance in Proteins. *Chem. Soc. Rev.* **1998**, *27*, 31−41. (b) Senge, M. O.; MacGowan, S. A.; O'Brien, J. M. Conformational Control of Cofactors in Nature - the Influence of Protein-Induced Macrocycle Distortion on the Biological Function of Tetrapyrroles. *Chem. Commun.* **2015**, *51*, 17031−17063.

(13) (a) Arnold, L.; Müllen, K. Modifying the Porphyrin Core—a Chemist's Jigsaw. *J. Porphyrins Phthalocyanines* **2011**, *15*, 757−779. (b) Brückner, C.; Akhigbe, J.; Samankumara, L. Syntheses and Structures of Porphyrin Analogues Containing Non-Pyrrolic Heterocycles. In *Handbook of Porphyrin Science*; Kadish, K. M., Smith, K. M., Guilard, R., Eds.; World Scientific: River Edge, NY, 2014; Vol. *31*, pp 1−276. (c) Szyszko, B.; Latos-Grazynski, L. Core Chemistry and Skeletal Rearrangements of Porphyrinoids and Metalloporphyrinoids. *Chem. Soc. Rev.* **2015**, *44*, 3588−3616. (d) Costa, L. D.; Costa, J. I.; Tome, A. C. Porphyrin Macrocycle Modification: Pyrrole Ring-Contracted or -Expanded Porphyrinoids. *Molecules* **2016**, *21*, 320. (e) Brückner, C. The Breaking and Mending of *meso*-Tetraarylporphyrins: Transmuting the Pyrrolic Building Blocks. *Acc. Chem. Res.* **2016**, *49*, 1080−1092.

(14) Lash, T. D. Out of the Blue! Azuliporphyrins and Related Carbaporphyrinoid Systems. *Acc. Chem. Res.* **2016**, *49*, 471−482.

(15) (a) Crossley, M. J.; King, L. G. Novel Heterocyclic Systems from Selective Oxidation at the B-Pyrrolic Position of Porphyrins. *J. Chem. Soc., Chem. Commun.* **1984**, 920−922. (b) Gouterman, M.; Hall, R. J.; Khalil, G. E.; Martin, P. C.; Shankland, E. G.; Cerny, R. L. Tetrakis(pentafluorophenyl)porpholactone. *J. Am. Chem. Soc.* **1989**, *111*, 3702−3707. (c) Jayaraj, K.; Gold, A.; Austin, R. N.; Ball, L. M.; Terner, J.; Mandon, D.; Weiss, R.; Fischer, J.; DeCian, A.; Bill, E.; Müther, M.; Schünemann, V.; Trautwein, A. X. Compound I and Compound II Analogues from Porpholactones. *Inorg. Chem.* **1997**, *36*, 4555−4566. (d) Yu, Y.; Lv, H.; Ke, X.; Yang, B.; Zhang, J.-L. Ruthenium-Catalyzed Oxidation of the Porphyrin *β,β′*-Pyrrolic Ring: A General and Efficient Approach to Porpholactones. *Adv. Synth. Catal.* **2012**, *354*, 3509−3516. (e) Brückner, C.; Ogikubo, J.; McCarthy, J. R.; Akhigbe, J.; Hyland, M. A.; Daddario, P.; Worlinsky, J. L.; Zeller, M.; Engle, J. T.;

DOI: 10.1021/acs.inorgchem.7b00799
Inorg. Chem. 2017, 56, 11490−11502

Ziegler, C. J.; Ranaghan, M. J.; Sandberg, M. N.; Birge, R. R. *meso*-Arylporpholactones and Their Reduction Products. *J. Org. Chem.* **2012**, *77*, 6480−6494. (f) Sharma, M.; Meehan, E.; Mercado, B. Q.; Brückner, C. *β*-Alkyloxazolochlorins: Revisiting the Ozonation of Octaalkylporphyrins, and Beyond. *Chem. - Eur. J.* **2016**, *22*, 11706−11718.

(16) (a) Lash, T. D. Synthesis of Novel Porphyrinoid Chromophores. In *The Porphyrin Handbook*; Kadish, K. M., Smith, K. M., Guilard, R., Eds.; Academic Press: San Diego, 2000; Vol. 2, pp 125−200. (b) Adams, K. R.; Bonnett, R.; Burke, P. J.; Salgado, A.; Valles, M. A. The 2,3-Secochlorin-2,3-Dione System. *J. Chem. Soc., Chem. Commun.* **1993**, 1860−1861. (c) Ryppa, C.; Niedzwiedzki, D.; Morozowich, N. L.; Srikanth, R.; Zeller, M.; Frank, H. A.; Brückner, C. Stepwise Conversion of Two Pyrrole Moieties of Octaethylporphyrin to Pyridin-3-Ones: Synthesis, Mass Spectral, and Photophysical Properties of Mono and Bis(oxypyri)porphyrins. *Chem. - Eur. J.* **2009**, *15*, 5749−5762. (d) Banerjee, S.; Zeller, M.; Brückner, C. *meso*-Tetraphenylporphyrin-Derived Oxypyriporphyrin, Oxypyrichlorin, and Thiomorpholinochlorin, as Their Ni(II) Complexes. *J. Porphyrins Phthalocyanines* **2012**, *16*, 576−588. (e) Lash, T. D.; Bergman, K. M. Further Observations on Conformational and Substituent Effects in Acid-Catalyzed ″3 + 1″ Cyclizations of Tripyrranes with Aromatic Dialdehydes. *J. Org. Chem.* **2012**, *77*, 9774−9783. (f) Lash, T. D.; Chaney, S. T. Conjugated Macrocycles Related to the Porphyrins. 6. Oxypyriporphyrin, the First Fully Aromatic Porphyrinoid Macrocycle with a Pyridine Subunit. *Chem. - Eur. J.* **1996**, *2*, 944−948.

(17) Callot, H. J.; Schaeffer, E. Homologation Directe Du Cycle Des Porphyrines Par Les Diazoalcanes (Direct Homologation of Porphyrin Rings by Diazoalkanes). *Tetrahedron* **1978**, *34*, 2295−2300.

(18) (a) Brückner, C.; Rettig, S. J.; Dolphin, D. Formation of a *meso*-Tetraphenylsecochlorin and a Homoporphyrin with a Twist. *J. Org. Chem.* **1998**, *63*, 2094−2098. (b) Daniell, H. W.; Brückner, C. Enantiomeric Resolution of a Ruffled Porphyrinoid. *Angew. Chem., Int. Ed.* **2004**, *43*, 1688−1691. (c) McCarthy, J. R.; Jenkins, H. A.; Brückner, C. Free Base *meso*-Tetraaryl-Morpholinochlorins and Porpholactone from *meso*-Tetraaryl-2,3-Dihydroxy-Chlorin. *Org. Lett.* **2003**, *5*, 19−22. (d) Brückner, C.; Götz, D. C. G.; Fox, S. P.; Ryppa, C.; McCarthy, J. R.; Bruhn, T.; Akhigbe, J.; Banerjee, S.; Daddario, P.; Daniell, H. W.; Zeller, M.; Boyle, R. W.; Bringmann, G. Helimeric Porphyrinoids: Stereostructure and Chiral Resolution of meso-Tetraarylmorpholinochlorins. *J. Am. Chem. Soc.* **2011**, *133*, 8740−8752.

(19) Samankumara, L. P.; Wells, S.; Zeller, M.; Acuña, A. M.; Röder, B.; Brückner, C. Expanded Bacteriochlorins. *Angew. Chem., Int. Ed.* **2012**, *51*, 5757−5760.

(20) Guberman-Pfeffer, M. J.; Greco, J. A.; Samankumara, L. P.; Zeller, M.; Birge, R. R.; Gascón, J. A.; Brückner, C. Bacteriochlorins with a Twist: Discovery of a Unique Mechanism to Red-Shift the Optical Spectra of Bacteriochlorins. *J. Am. Chem. Soc.* **2017**, *139*, 548−560.

(21) Brückner, C.; Hyland, M. A.; Sternberg, E. D.; MacAlpine, J.; Rettig, S. J.; Patrick, B. O.; Dolphin, D. Preparation of [meso-Tetraphenylchlorophinato]Nickel(II) by Stepwise Deformylation of [*meso*-Tetraphenyl-2,3-Diformylsecochlorinato]Nickel(II): Conformational Consequences of Breaking the Structural Integrity of Nickel Porphyrins. *Inorg. Chim. Acta* **2005**, *358*, 2943−2953.

(22) (a) Barkigia, K. M.; Renner, M. W.; Furenlid, L. R.; Medforth, C. J.; Smith, K. M.; Fajer, J. Crystallographic and Exafs Studies of Conformationally Designed Nonplanar Nickel(II) Porphyrins. *J. Am. Chem. Soc.* **1993**, *115*, 3627−3635. (b) Senge, M. O. Highly Substituted Porphyrins. In *The Porphyrin Handbook*; Kadish, K. M., Smith, K. M., Guilard, R., Eds.; Academic Press: San Diego, 2000; Vol. *1*, pp 239−347. (c) Senge, M. O.; Renner, M. W.; Kalisch, W. W.; Fajer, J. Molecular Structure of (5,10,15,20-Tetrabutyl-2,3,7,8,12,13,17,18-Octaethylporphyrinato)nickel(II)−Correlation of Nonplanarity with Frontier Orbital Shifts. *Dalton* **2000**, 381−385. (d) Fajer, J. Structural Effects in Chemistry and Biology. *J. Porphyrins Phthalocyanines* **2000**, *4*, 382−385. (e) Haddad, R. E.; Gazeau, S.; Pécaut, J.; Marchon, J.-C.; Medforth, C. J.; Shelnutt, J. A. Origin of the Red Shifts in the Optical Absorption Bands of Nonplanar Tetraalkylporphyrins. *J. Am. Chem. Soc.* **2003**, *125*, 1253−1268.

(23) (a) Kratky, C.; Waditschatka, R.; Angst, C.; Johansen, J. E.; Plaquevent, J. C.; Schreiber, J.; Eschenmoser, A. Die Sattelkonformation Der Hydroporphinoiden Ni(II)-Komplexe: Struktur, Ursprung, Und Stereochemische Konsequenzen. *Helv. Chim. Acta* **1985**, *68*, 1312−1337. (b) Gudowska-Nowak, E.; Newton, M.; Fajer, J. Conformational and Environmental Effects on Bacteriochlorophyll Optical Spectra: Correlations of Calculated Spectra with Structural Results. *J. Phys. Chem.* **1990**, *94*, 5795−5801. (c) Linnanto, J.; Korppi-Tommola, J. Structural and Spectroscopic Properties of Mg-Bacteriochlorin and Methyl Bacteriochlorophyllides *a*, *b*, *g*, and *h* Studied by Semiempirical, *ab initio*, and Density Functional Molecular Orbital Methods. *J. Phys. Chem. A* **2004**, *108*, 5872−5882. (d) Zucchelli, G.; Brogioli, D.; Casazza, A. P.; Garlaschi, F. M.; Jennings, R. C. Chlorophyll Ring Deformation Modulates Q_y Electronic Energy in Chlorophyll-Protein Complexes and Generates Spectral Forms. *Biophys. J.* **2007**, *93*, 2240−2254. (e) Wondimagegn, T.; Ghosh, A. Ruffling Deformations of Nickel(II) and Zinc(II) Hydroporphyrin and Chlorophin Complexes: Implications Fro F430, the Nickel Tetrapyrrole Cofactor of Methylcoenzyme M Reductase. *J. Phys. Chem. B* **2000**, *104*, 10858−10862. (f) Senge, M. O.; Smith, N. W.; Smith, K. M. Structural Investigation of Nickel(II) Bacteriopetroporphyrins Related to the Bacteriochlorophylls-C and Bacteriochlorophylls-D - Evidence for Localized Conformational Distortion in the C-Series. *Inorg. Chem.* **1993**, *32*, 1259−1265. (g) MacGowan, S. A.; Senge, M. O. Conformational Control of Cofactors in Nature—Functional Tetrapyrrole Conformations in the Photosynthetic Reaction Centers of Purple Bacteria. *Chem. Commun.* **2011**, *47*, 11621−11623. (h) MacGowan, S. A.; Senge, M. O. Contribution of Bacteriochlorophyll Conformation to the Distribution of Site-Energies in the Fmo Protein. *Biochim. Biophys. Acta, Bioenerg.* **2016**, *1857*, 427−442. (i) Bednarczyk, D.; Dym, O.; Prabahar, V.; Peleg, Y.; Pike, D. H.; Noy, D. Fine Tuning of Chlorophyll Spectra by Protein-Induced Ring Deformation. *Angew. Chem., Int. Ed.* **2016**, *55*, 6901−6905.

(24) Samankumara, L. P.; Zeller, M.; Krause, J. A.; Brückner, C. Syntheses, Structures, Modification, and Optical Properties of *meso*-Tetraaryl-2,3-Dimethoxychlorin, and Two Isomeric *meso*-Tetraaryl-2,3,12,13-Tetrahydroxybacteriochlorins. *Org. Biomol. Chem.* **2010**, *8*, 1951−1965.

(25) Buchler, J. W. Synthesis and Properties of Metalloporphyrins. In *The Porphyrins*; Dolphin, D., Ed.; Academic Press: New York, 1978; Vol. *1*, pp 389−483.10.1016/B978-0-12-220101-1.50017-2

(26) Dean, M. L.; Schmink, J. R.; Leadbeater, N. E.; Brückner, C. Microwave-Promoted Insertion of Group 10 Metals into Free Base Porphyrins and Chlorins: Scope and Limitations. *Dalton Trans.* **2008**, 1341−1345.

(27) Lindsey, J. S.; Prathapan, S.; Johnson, T. E.; Wagner, R. W. Porphyrin Building Blocks for Modular Construction of Bioorganic Model Systems. *Tetrahedron* **1994**, *50*, 8941−8968.

(28) Mitevski, O.; Dechert, S.; Brückner, C.; Meyer, F. Siamese-Twin Porphyrins: Variation of Two meso-Aryl Groups. *Eur. J. Inorg. Chem.* **2016**, *2016*, 4814−4819.

(29) Senge, M. O. Database of Tetrapyrrole Crystal Structure Determinations. In *The Porphyrin Handbook*; Kadish, K. M., Smith, K. M., Guilard, R., Eds.; Academic Press: San Diego, 2000; Vol. *10*, pp 1−218.

(30) Shannon, R. D. Revised Effective Ionic Radii and Systematic Studies of Interatomic Distances in Halides and Chalcogenides. *Acta Crystallogr., Sect. A: Cryst. Phys., Diffr., Theor. Gen. Crystallogr.* **1976**, *32*, 751−767.

(31) Chimera: Molecular Graphics Images were Produced Using the UCSF Chimera Package (V. 1.11.1, 2016): Pettersen, E. F.; Goddard, T. D.; Huang, C. C.; Couch, G. S.; Greenblatt, D. M.; Meng, E. C.; Ferrin, T. E. UCSF Chimera: A Visualization System for Exploratory Research and Analysis. *J. Comput. Chem.* **2004**, *25*, 1605−1612.

(32) Jentzen, W.; Song, X.-Z.; Shelnutt, J. A. Structural Characterization of Synthetic and Protein-Bound Porphyrins in Terms of the Lowest-Frequency Normal Coordinates of the Macrocycle. *J. Phys. Chem. B* **1997**, *101*, 1684−1699.

DOI: 10.1021/acs.inorgchem.7b00799
Inorg. Chem. 2017, 56, 11490−11502

(33) Shelnutt, J. A. Molecular Simulations and Normal-Coordinate Structural Analysis of Porphyrins and Heme Proteins. In *The Porphyrin Handbook*; Kadish, K. M., Smith, K. M., Guilard, R., Eds.; Academic Press: San Diego, 2000; Vol. 7, pp 167−223.
(34) Gouterman, M. Optical Spectra and Electronic Structure of Porphyrins and Related Rings. In *The Porphyrins*; Dolphin, D., Ed.; Academic Press: New York, 1978; Vol. 3, Part A, pp 1−165.
(35) Stolzenberg, A. M.; Stershic, M. T. Reductive Chemistry of Nickel Hydroporphyrins. Evidence for a Biologically Significant Difference Porphyrins, Hydroporphyrins, and Other Tetrapyrroles. *J. Am. Chem. Soc.* **1988**, *110*, 6391−6402.
(36) Zhong, Y.-L.; Shing, T. K. M. Efficient and facile Glycol Cleavage Oxidation Using Improved Silica Gel-Supported Sodium Metaperiodate. *J. Org. Chem.* **1997**, *62*, 2622−2624.
(37) Sheldrick, G. M. *SHELXTL*; University of Göttingen: Göttingen, Germany, 2016.

DOI: 10.1021/acs.inorgchem.7b00799
Inorg. Chem. 2017, 56, 11490−11502